

# Global $R^*$

A. Cesa-Bianchi<sup>†</sup>

Bank of England  
CEPR and CfM

R. Harrison<sup>‡</sup>

Bank of England  
and CfM

R. Sajedi<sup>§</sup>

Bloomberg

September 17, 2024

## Abstract

This paper develops a structural model to study the global trend real interest rate, “Global  $R^*$ ”. We focus on five potential drivers: productivity growth, population growth, longevity, government debt, and the relative price of capital. We employ a recursive simulation method in which beliefs about long-run trends are updated gradually. The simulations are guided by estimates of the global trend component of each driver derived from a panel dataset of 31 countries from 1950 to 2020. Global  $R^*$  rises until the mid-1970s before declining by around 3 percentage points. The decline is driven by slowing productivity growth and increasing longevity.

**Key Words:** Long-Run Interest Rates, Structural Change, Macroeconomic Policy

**JEL Codes:** E22, E43, E60

---

We are grateful to two anonymous referees, Emi Nakamura, Jesús Fernández-Villaverde, Andrea Ferrero, Pierre-Olivier Gourinchas, Şebnem Kalemli-Özcan, Thomas Laubach, Miguel León-Ledesma, Nick McLaren, Marcel Peruffo, Alan Taylor, Gregory Thwaites, and participants at RES 2019, EcoMod 2022, the ECB-BOE-BOJ Joint Research Workshop 2022, 30th CEPR ESSIM, PSE Macro Days 2023, 17th Dynare Conference, and seminars at Reserve Bank of Australia and Banque de France, for useful comments and suggestions. We would like to thank Caroline Butler and Veronica Veggente for outstanding research assistance. This paper was previously circulated as “Decomposing the Drivers of Global  $R^*$ ”. The views expressed in this paper are those of the authors and do not necessarily represent the views of the Bank of England or its committees.

<sup>†</sup>Email: [ambrogio.cesa-bianchi@bankofengland.co.uk](mailto:ambrogio.cesa-bianchi@bankofengland.co.uk)

<sup>‡</sup>Email: [richard.harrison@bankofengland.co.uk](mailto:richard.harrison@bankofengland.co.uk)

<sup>§</sup>Email: [rana.sajedi@gmail.com](mailto:rana.sajedi@gmail.com)

# 1 Introduction

Recent increases in government bond returns around the world, following a multi-decade decline, have intensified the debate on the long-run prospects for interest rates. Are the previous trends reversing or will we return to the era of low rates as the current shocks subside? Answering this question requires an assessment of the underlying forces driving secular movements in interest rates. In this paper we investigate these forces, emphasizing their global nature and focusing on five potential drivers: productivity growth, population growth, longevity, government debt, and the relative price of capital.

Within a standard macroeconomic framework, secular movements in real interest rates are determined by the factors that drive the supply and demand for capital. Over the long run, when capital can move freely across countries, there exists a single interest rate that clears the global capital market. This global trend real interest rate, which we call ‘Global  $R^*$ ’, acts as an anchor for domestic interest rates. Therefore, studying the factors that drive global wealth and capital accumulation is crucial for understanding interest rate trends around the world.

We develop a structural model to study the drivers of Global  $R^*$  since 1950. Following an initial increase, we find that Global  $R^*$  fell by more than 3 percentage points between the late 1970s and 2020. In the early part of the simulation, higher productivity growth and population growth (i.e., the ‘baby boom’) account for the rise of Global  $R^*$ . The subsequent decline is driven by falling productivity growth and increased longevity. Indeed these two drivers alone more than account for the total fall, while the other drivers have had much smaller, and sometimes partially offsetting, effects on Global  $R^*$ . These results suggest that, without a substantial reversal in the trends in productivity growth or longevity, or new drivers emerging to offset these trends, Global  $R^*$  is likely to remain low.

Our structural model is designed to parsimoniously capture the effects of slow-moving trends in the five drivers, abstracting from business-cycle fluctuations. We treat the world as a single large (closed) economy, populated by overlapping generations of finitely-lived households that face age-specific mortality rates. The model is solved around a balanced-

growth path, allowing for steady-state population and productivity growth. Households save using both the productive capital stock, the relative price of which varies over time, and an exogenous stock of bonds issued by the fiscal authority. We allow a fixed premium between the rate of return on capital and the return on the government bond (i.e., the real interest rate).<sup>1</sup> Conditional on the (exogenous) global trends in each of the drivers, the equilibrium response of the real interest rate in the model represents a simulated path for Global  $R^*$ .

To guide these simulations we use a panel dataset of 31 countries from 1950 to 2020. We show that our group of countries can be regarded as a good approximation to the single fully integrated closed economy. The dynamic path of each driver is estimated by extracting the low-frequency common component for each series, representing their long-run global trends.<sup>2</sup> Furthermore, we use a reduced-form empirical estimate of Global  $R^*$ , based on the same group of countries, to calibrate the model and to set the initial level of the interest rate at the start of the simulations.

The model simulations are constructed using a recursive methodology that captures slow-moving beliefs about long-term trends, as an alternative to the commonly used perfect-foresight approach. Since our simulations span seventy years of substantial structural change, the assumption that agents fully anticipate the future paths of the drivers is implausible and at odds with evidence of persistent errors in forecasting low-frequency changes in the drivers. Our recursive approach instead assumes that the beliefs about the future evolution of the drivers are only partially updated each period. Compared with a perfect-foresight simulation, this implies a larger initial rise and faster subsequent fall of Global  $R^*$ , resulting in a simulated path that is closer to the empirical estimate.

Our paper is related to several strands of the literature. We move beyond existing work using structural models by considering a range of potential drivers of  $R^*$ , at the global level, within a single framework.<sup>3</sup> Farhi and Gourio (2018), Eggertsson et al.

---

<sup>1</sup>We therefore focus on the macroeconomic drivers of long-run real rates, abstracting from financial factors that affect bond premia. See Davis et al. (2023) for a recent discussion of this distinction and evidence in favor of the macro approach.

<sup>2</sup>The availability of data for our full panel is the main constraint on the choice of drivers that we incorporate. Appendix E discusses the potential drivers missing from our framework, including risk premia, in more detail.

<sup>3</sup>Rachel and Smith (2017) was an early contribution on the determinants of the decline in global real

(2019), and [Platzer and Peruffo \(2022\)](#) undertake an exercise similar to ours, analyzing a similar set of drivers within a structural model, but focusing on the United States as a closed economy, thereby abstracting from the global nature of many of these trends. [Marx et al. \(2021\)](#), also carry out a similar exercise looking separately at the US and the Euro-area, and focusing on understanding the spread between risk-free rates and the return to capital. Conversely, studies of Global  $R^*$  have typically focused on a narrower subset of drivers or countries. For example, [Carvalho et al. \(2016\)](#) and [Lisack et al. \(2021\)](#) focus solely on the role of demographic drivers across advanced economies. Recently both [Rachel and Summers \(2019\)](#) and [Carvalho et al. \(2023\)](#) also emphasize the importance of the global dimension of  $R^*$ , with their analyses focusing on the role of various fiscal policy instruments and demographic factors, respectively.

Our results are also related to estimates of equilibrium real interest rates for individual countries. Many existing studies use closed-economy semi-structural models to estimate a higher-frequency concept of the equilibrium real interest rate: the real interest rate that stabilizes output at potential and inflation at target (see, for example, [Laubach and Williams, 2003](#); [Holston et al., 2017](#)). That framework typically assumes that the ‘short-term’ equilibrium interest rate is determined by cyclical domestic shocks. Our approach aims to identify the role of longer-term global trends. Therefore, we purposefully abstract from shorter-term deviations of an individual economy’s real interest rate from Global  $R^*$  and hence the effects of shocks on domestic equilibrium rates over shorter horizons. Nevertheless, over longer horizons, Global  $R^*$  acts as an anchor for domestic equilibrium real interest rates in open economies, so that estimates of Global  $R^*$  are important inputs to longer-term structural analysis, including the design of policy frameworks.<sup>4</sup>

Finally, our analysis complements and extends existing empirical estimates of global equilibrium real interest rates. Most closely related are the estimates of  $R^*$  at a global level produced by [Del Negro et al. \(2019\)](#) and [Kiley \(2020\)](#), who extract a common trend from their panels of 7 and 13 countries, respectively. Their estimates suggest that Global  $R^*$  fell by around 3 percentage points between 1980 and 2015. Our empirical estimate of Global  $R^*$  applies a variant of the [Del Negro et al. \(2019\)](#) approach to our larger panel,

---

interest rates, combining the results of several alternative models to derive a reduced-form decomposition.

<sup>4</sup>See [Bailey et al. \(2022\)](#) and [Obstfeld \(2023\)](#) for further discussion of this distinction.

and finds similar trends.

The rest of the paper is organized as follows. Section 2 lays out the structural model, while Section 3 describes the empirical measures of the global trends in the five drivers. Section 4 details the calibration and the recursive simulation method. Section 5 describes the results of the model simulations, including a comparison with the empirical estimate, and an assessment of the robustness of the baseline simulations. Section 6 concludes.

## 2 The Structural Model

This section provides an overview of the structural model used for our exploration of the global trend real interest rate. Full details are presented in Appendix A.

### 2.1 Timing and Overlapping-Generation Structure

Time is discrete and indexed by periods  $t = 1, \dots, \infty$ . The age of a household is indexed by  $\tau$  and each household enters the model at age  $\tau = 1$  and leaves with certainty at age  $\tau = T$ . Each time period in the model corresponds to 5 years and calibrated such that age  $\tau = 1$  corresponds to age 20-24. We set  $T = 14$  so that households leave the model with certainty at age 85-89.

Between ages  $\tau = 1$  and  $\tau = T$ , households face probabilistic mortality:  $\Pi_{t,\tau}$  denotes the probability that a household that was aged  $(\tau - 1)$  in period  $(t - 1)$  will survive to reach age  $\tau$  in period  $t$ . Note that  $\Pi_{t,1} = 1$  and  $\Pi_{t,T+1} = 0$  for all  $t$ .

### 2.2 Household Optimization

Each period, households maximize utility from consumption subject to their budget constraint. In period  $t$ , a household aged  $\tau$ , with existing assets  $a_{t-1,\tau-1}$  brought forward from the previous period, solves the following recursive maximization problem:

$$\max_{c_{t,\tau}, a_{t,\tau}} V(t, \tau, a_{t-1,\tau-1}) = \beta_\tau \frac{c_{t,\tau}^{1-\theta}}{1-\theta} + \mathbb{E}_t \left[ \Pi_{t+1,\tau+1} V(t+1, \tau+1, a_{t,\tau}) \right],$$

subject to:

$$c_{t,\tau} + a_{t,\tau} = \rho_\tau w_t + (1 + r_{t-1})a_{t-1,\tau-1} + \varpi_{t,\tau},$$

where  $\beta_\tau$  is an age-specific utility weight and  $\rho_\tau$  is age-specific (inelastic) labor supply.<sup>5</sup>  $\varpi_{t,\tau}$  is non-labor income that the households take as exogenous, and which will be defined below.  $w_t$  is the wage per effective unit of labor, and  $r_t$  is the net real interest rate paid out in period  $t + 1$  on assets accumulated in period  $t$ . We assume that households are born with no assets, and do not have any incentives to retain assets when  $\tau = T$ , so that  $a_{t,0} = a_{t,T} = 0$  for all  $t$ .<sup>6</sup>

This optimization leads to a set of  $(T - 1)$  Euler equations:

$$c_{t,\tau}^{-\theta} = \tilde{\beta}_\tau (1 + r_t) \mathbb{E}_t [\Pi_{t+1,\tau+1} c_{t+1,\tau+1}^{-\theta}] \quad \text{for } \tau = 1, \dots, T - 1.$$

where  $\tilde{\beta}_\tau \equiv \beta_{\tau+1}/\beta_\tau$  denotes the relative weights on utility at age  $\tau + 1$  and  $\tau$ . In this way,  $\tilde{\beta}_\tau$  corresponds to the more familiar notion of the household's degree of 'patience' at age  $\tau$ .

## 2.3 Firms

A monopolistic retailer buys  $Y_t$  units of an intermediate good and sells it as a final good with a net mark-up,  $\mu$ , over marginal cost. The price of the final good is normalized to 1, so that the relative price of the intermediate good is given by  $1/(1 + \mu)$ . The aggregate profit of the retailer, given by:

$$\mathcal{P}_t = \frac{\mu}{1 + \mu} Y_t,$$

is distributed to the households, as described below.

The intermediate good is produced with capital,  $K_{t-1}$ , brought forward from the

---

<sup>5</sup>We do not impose a fixed retirement age, but will calibrate  $\rho_\tau$  to match the observed pattern of labor supply of different age groups. Labor supply declines in old age, effectively capturing retirement decisions. Further details are provided in Section 4.2.

<sup>6</sup>Note that all savings are in the single private asset,  $a$ , and we abstract from any public pension or social security system.

previous period, and labor,  $L_t$ , using a CES production function:

$$Y_t = \left( \alpha K_{t-1}^{\frac{\sigma-1}{\sigma}} + (1-\alpha)(E_t L_t)^{\frac{\sigma-1}{\sigma}} \right)^{\frac{\sigma}{\sigma-1}},$$

where  $E_t$  is a labor-augmenting technological process with net growth rate  $e_t$ .

The intermediate-good-producing firm's profit maximization can be written as:

$$\max_{K_t, L_t} \frac{1}{1+\mu} Y_t - (r_t^k p_t^k K_{t-1} + w_t L_t),$$

where  $p_t^k$  is the relative price of capital,  $r_t^k$  is the rental rate of capital, and  $w_t$  is the wage per units of labor. This gives the first-order conditions:

$$\begin{aligned} r_t^k &= \frac{1}{1+\mu} \alpha \frac{1}{p_t^k} \left( \frac{Y_t}{K_{t-1}} \right)^{\frac{1}{\sigma}}, \\ w_t &= \frac{1}{1+\mu} (1-\alpha) E_t \left( \frac{Y_t}{L_t} \right)^{\frac{1}{\sigma}}. \end{aligned}$$

## 2.4 Government

The government issues a stock of debt,  $G_t$ , on which it pays interest,  $r_t$ . It also levies a lump-sum tax on households,  $\mathcal{T}_t$ . Hence the government budget constraint is given by:

$$G_t = (1 + r_{t-1})G_{t-1} - \mathcal{T}_t.$$

## 2.5 Financial Intermediary

At the end of each period, a financial intermediary takes the aggregate assets of the households, promising a net return of  $r_t$  per unit in the next period. They use part of this asset to buy the stock of government debt, which provides this safe rate of return.

The remaining assets are turned into capital goods, and stored for production in the next period. The financial intermediary earns the rental rate, net of depreciation,  $(1 + r_{t+1}^k - \delta)$ , on this capital, as well as any capital gains from changes in the relative

price of capital,  $p_{t+1}^k/p_t^k$ .

We assume that there is a fixed spread,  $\phi$ , between the return on capital and the risk-free rate paid out to households:

$$1 + r_t = (1 + r_{t+1}^k - \delta) \frac{p_{t+1}^k}{p_t^k} - \phi.$$

This spread is treated as a resource cost to the economy, which can also be viewed as an additional cost to the financial intermediary, such as the cost of storing capital.

## 2.6 Aggregation

We complete the description of the model by defining some aggregate concepts and market-clearing conditions.

**Population growth.** Let  $N_{t,\tau}$  be the size of the cohort aged  $\tau$  at time  $t$ . The law of motion of cohort sizes is given by:

$$N_{t,\tau} = \Pi_{t,\tau} N_{t-1,\tau-1} \quad \text{for } \tau = 2, \dots, T.$$

We denote the net growth rate of consecutive cohorts entering the model as:

$$n_t \equiv \frac{N_{t,1} - N_{t-1,1}}{N_{t-1,1}}.$$

Though we will refer to  $n$  as the “population growth rate”, note that this is not the fertility or birth rate, nor the growth rate of the aggregate population, except in steady state.

**Labor.** Total labor supply is given by:

$$L_t = \sum_{\tau=1}^T N_{t,\tau} \rho_{\tau}.$$

**Asset markets.** The aggregate assets of the household given to the financial intermediary are either used to buy the stock of government debt, or turned into capital:

$$p_t^k K_t + G_t = \sum_{\tau=1}^T N_{t,\tau} a_{t,\tau}.$$

Households that die between periods leave their assets, along with the return, as accidental bequests. Aggregate accidental bequests are given by:

$$\mathcal{B}_t = (1 + r_{t-1}) \sum_{\tau=1}^T (1 - \Pi_{t,\tau+1}) N_{t-1,\tau} a_{t-1,\tau}.$$

**Non-labor income.** The non-labor income of the household,  $\varpi_{t,\tau}$ , comprises of the monopolistic profit of the retailer, the accidental bequests, less the lump-sum taxes paid to the government. These objects have thus far been defined as aggregates in each period:  $\mathcal{P}_t$ ,  $\mathcal{B}_t$  and  $\mathcal{T}_t$ . To account for how these aggregates are distributed among the different generations, we introduce the parameters  $\{\mathbf{p}_\tau, \mathbf{b}_\tau, \mathbf{t}_\tau\}_{\tau=1}^T$  such that the total non-labor income of each generation  $\tau$  can be written as:

$$N_{t,\tau} \varpi_{t,\tau} = \mathbf{p}_\tau \mathcal{P}_t + \mathbf{b}_\tau \mathcal{B}_t - \mathbf{t}_\tau \mathcal{T}_t,$$

with  $\sum_{\tau=1}^T \mathbf{p}_\tau = \sum_{\tau=1}^T \mathbf{b}_\tau = \sum_{\tau=1}^T \mathbf{t}_\tau = 1$ .

### 3 Drivers of Global $R^*$

The structural model has five exogenous processes, which we refer to as the ‘drivers’. These are: (i)  $e_t$ , the growth rate of the labor-augmenting technology; (ii)  $n_t$ , the population growth rate; (iii)  $\Pi_{t,\tau}$  for  $\tau = 2, \dots, T$ , the survival probabilities at each age; (iv)  $GY_t \equiv G_t/Y_t$ , the government debt to GDP ratio; and (v)  $p_t^k$ , the relative price of capital goods. In what follows, we denote the vector of the drivers in each point in time as  $d_t \equiv [e_t, n_t, \Pi_{t,2}, \dots, \Pi_{t,T}, GY_t, p_t^k]'$ . These five drivers determine equilibrium allocations and prices, including the interest rate,  $r_t$ . By simulating the model response to slow-

moving global trends in the drivers, the path of  $r_t$  can be interpreted as a simulation of Global  $R^*$ .

This section describes the construction of observable proxies for these slow-moving global trends in the exogenous processes in  $d_t$ , based on a large panel of countries.

We abstract from several additional drivers that have been argued to have important effects on real interest rates. These drivers cannot be incorporated because of the difficulty in building a reliable panel of data for the countries and time period that we study. In Appendix E we draw on existing literature to discuss the likely effects of these additional drivers on Global  $R^*$ .

### 3.1 High-Income Country Group

We estimate the drivers of Global  $R^*$  as common factors from a large large panel data set for 31 ‘high-income’ countries. This group of countries can be regarded as a good approximation to the single world economy in our structural model for two reasons: it is highly financially integrated and it has a small and stable current account position with the rest of the world.

Figure 1 demonstrates that the countries in our data set have a consistently high, and increasing, degree of capital account openness, based on a GDP-weighted measure of the index developed by Chinn and Ito (2006, 2008).<sup>7</sup> In contrast, the median openness of the rest of the countries in their sample is significantly lower throughout this time period.

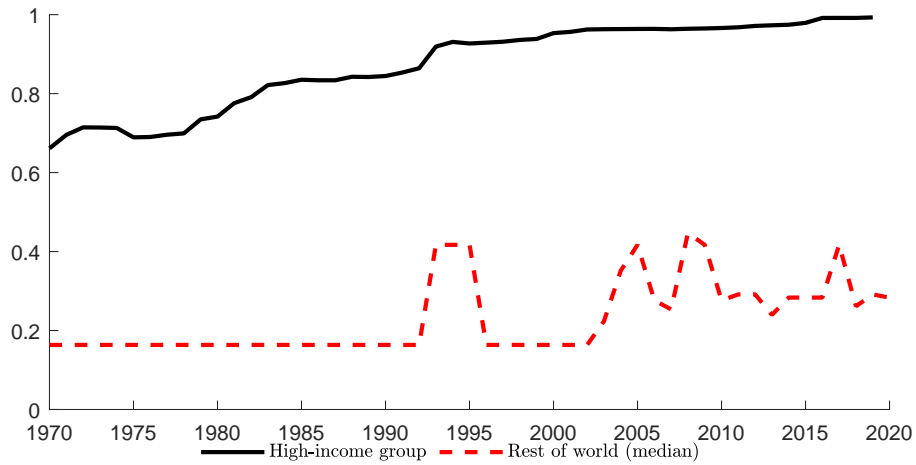
The average current-account-to-GDP ratio for this group of countries is small, 0.3% on average over the same time period and with no obvious trend. While this does not take into account bilateral current-account positions within countries in the sample, we note that our group of countries overlaps substantially with that studied by Rachel and Summers (2019).<sup>8</sup> They similarly argue that such a group of countries can be regarded

---

<sup>7</sup>Our full sample also includes the ‘Bretton Woods’ era at the start of the sample, a period that is largely absent from Figure 1 because of data limitations. That regime is one in which exchange rate and capital controls were generally more prevalent and so we would expect global capital market integration to have been lower during that period. However, judging the true degree of international financial market openness during that period requires careful analysis of a broad range of factors (Bordo et al., 1998).

<sup>8</sup>The groups have 27 countries in common and those countries account for 96% of the GDP of our

**Figure 1** Capital account openness



NOTE. The figure shows the normalized index of capital account openness developed by Chinn and Ito (2006, 2008) (on a PPP GDP-weighted basis).

as a “single, fully integrated economy” by virtue of its consolidated current-account dynamics.<sup>9</sup>

### 3.2 Productivity Growth, Government Debt, and the Relative Price of Capital

We start from country-level data for three of our drivers. Specifically, we obtain data on the stock of government debt from IMF Global Debt Database, the relative price of capital goods from the Penn World Tables (PWT), and the growth rate of labor-augmenting technology from Ziesemer (2021). The data are at annual frequency and cover the period from 1951 to 2020.<sup>10</sup> Appendix C provides additional details on the sources of the data.

To map the data to the model for these drivers, we proceed in three steps. First, we extract a common (or ‘global’) component from the country-level data. We approximate the global component by exploiting our large cross-section of countries and us-

---

‘high income’ group.

<sup>9</sup>Appendix C provides full details and further discussion of our country group.

<sup>10</sup>We exclude data for 2020 to avoid the large movements induced by the Covid-19 shock. We do so by re-scaling the data for the four-year period 2016–2019 and interpret it as data for 2016–2020.

ing cross-sectional (weighted) averages. As shown in [Pesaran \(2006\)](#), when the number of cross-sectional units is large, cross-sectional averages can approximate common factors in a similar way to principal components or other more sophisticated techniques.<sup>11</sup> For the calculation of weighted averages we use time-varying GDP weights from PWT (expenditure-side real GDP at current PPPs, in mil. 2017US\$).

Second, given our focus on slow-moving dynamics, we abstract from cyclical fluctuations and extract the low-frequency movements from the estimated global factors using an HP filter with a high value for the smoothing parameter  $\lambda$  (as, for example, in [Ferreira and Shousha, 2021](#)). Specifically, we set  $\lambda = 1,000$ . This choice is based on prior beliefs about the volatility of the trend component of the drivers. Lower values of the smoothing parameter, as commonly employed to recover the *cyclical* component of annual data, imply implausible values for the volatility of shocks to the trend.<sup>12</sup>

Third, we adjust the data to match the calibration of the model, in which each discrete time period is assumed to be 5 years. We employ the convention that the first period in the model simulations corresponds to 1951-1955 in the data, the second period corresponds to 1956-1960, and so on. The annual growth rate of the labor-augmenting technology,  $e_t$ , is compounded to compute a 5-year growth rate. For government debt to GDP,  $GY_t$ , we take the value of the debt to annual GDP at the end of each 5-year period in the data, and divide it by 5 to obtain the 5-year ratio, consistent with the end-of-period definition in the model. For the relative price of capital,  $p_t^k$ , we take an average of the annual values within each 5-year period.

Figure 2 plots the resulting drivers of Global  $R^*$ , derived from the procedure described above. The yellow line plots the common factors obtained by means of cross-sectional weighted averages and the blue line with circles plots the trend component obtained with the HP filter. For readability, the drivers are re-scaled to be in yearly space.<sup>13</sup> The

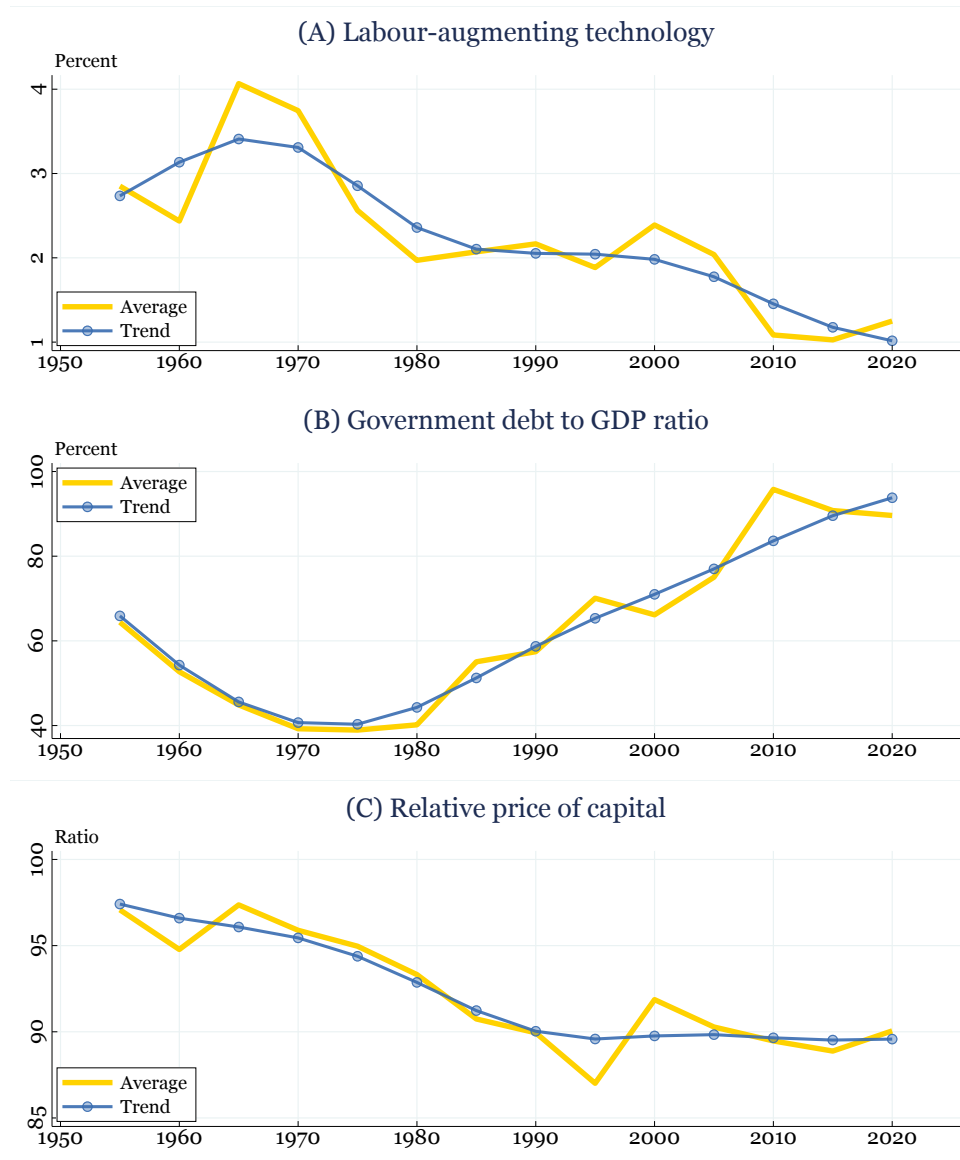
---

<sup>11</sup>While a large cross-section is the key assumption to obtain this result, some additional regularity conditions on the weights and the factor loadings are also needed. See [Pesaran \(2006\)](#).

<sup>12</sup>Ideally, the choice of  $\lambda$  should be adjusted so that it reflects prior knowledge on the length of the cycle. However, the smoothing parameter also affects the volatility of the trend – a consequence of the fact that the HP filter does not contain an explicit model of both the trend and the cycle. As a result, there is also a link between the prior for the variance of trend innovations and the HP smoothing parameter.

<sup>13</sup>For the labor-augmenting technological growth we plot the average growth rate over each 5-year

**Figure 2** Productivity Growth, Government Debt, and the Relative Price of Capital



NOTE. The figure plots the observable proxies for the productivity growth, government debt, and relative price of capital exogenous processes. The yellow line plots the common factors obtained with cross-sectional weighted averages of the observables, while the blue line with circles plots the trend component, obtained with the HP filter. Sample period: five-year periods from 1955 to 2020, where ‘1955’ corresponds to the period 1951-1955, and ‘2020’ corresponds to the period 2016-2019.

figure highlights a few secular trends that are common to the large group of economies we consider: (i) after increasing at the start of the sample, productivity growth has been declining steadily since the mid-1960s; (ii) government debt fell steadily until the mid-1970s, and has been trending upwards since then; (iii) the relative price of capital fell

period; for government debt over GDP we plot the stock of government debt over annual GDP at the end of the 5-year period; the relative price of capital requires no re-scaling.

steadily from 1955 and has stabilized since the 1990s.

### 3.3 Population Growth and Longevity

The two remaining drivers, population growth rates and survival probabilities, are treated separately. We obtain data on aggregate population numbers for our group of 31 countries by age group at 5-year frequency, from the UN World Population Prospects. This gives us the total number of people in our group of countries, in each 5-year age cohort, at the end of each 5-year period from 1955-2020. In line with the calibration of the model, we consider the age groups starting from 20-24 years old up to 85-89 years old.

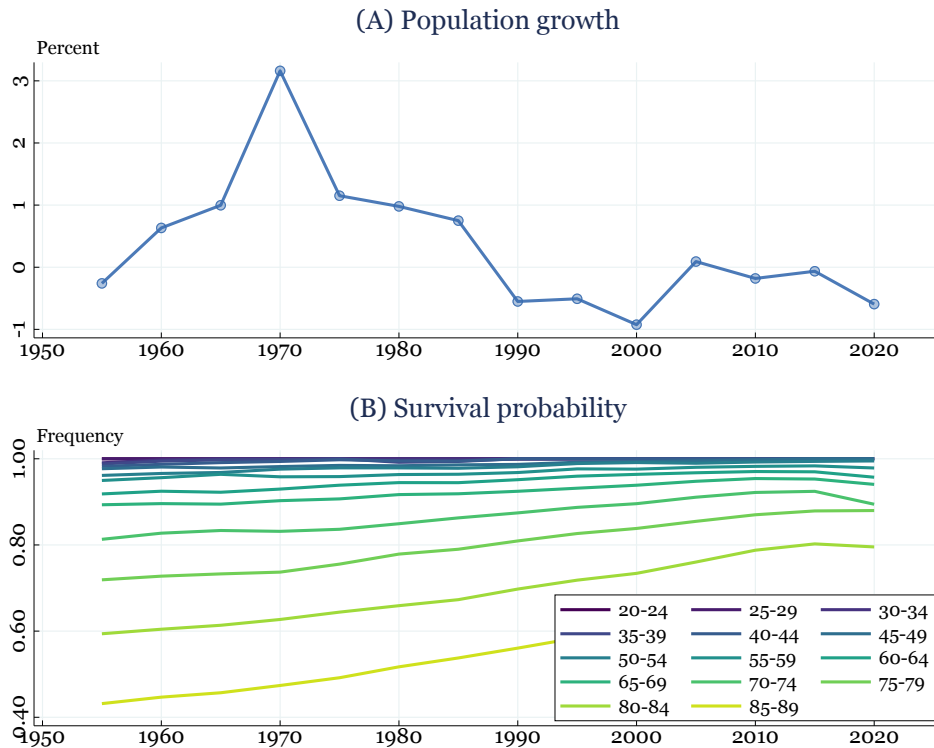
These data correspond directly to  $N_{t,\tau}$  in the model. Therefore, from this raw population data, we can calculate  $n_t$  as the net growth rate of consecutive 20-24 year old cohorts, and  $\Pi_{\tau,t}$  as the change in the size of a given cohort over time. We do not detrend these series since demographic trends are inherently slow moving, and therefore only relevant for long-run concepts of equilibrium interest rates. That is, short-run changes in population growth and survival probabilities are unlikely to have a material impact on equilibrium interest rates. We therefore assume that the observed evolution of population growth and cohort-specific survival probabilities coincide with the trend.

Figure 3 plots the resulting drivers of Global  $R^*$ , derived from the procedure described above. In panel (A), the blue line with circles plots the population growth rate of the high income group at the 5-year frequency. In panel (B) each line plots the evolution over time of the survival probability for each cohort. For readability, the drivers are re-scaled to be in yearly space.<sup>14</sup> The figure highlights two key trends: (i) after peaking in 1960, population growth has slowed down significantly, and was particularly low in the 1990s; (ii) longevity, as measured by the survival probabilities, has dramatically increased over time, in particular for those aged over 65.

---

<sup>14</sup>For population growth, we plot the average growth rate over each 5-year period. The survival probability requires no re-scaling.

**Figure 3** Population Growth and Longevity



NOTE. The figure plots the observable proxies for the population growth and survival probabilities exogenous processes. In panel (A), the blue line with circles plots the population growth rate of the high income group at 5-year frequency. In panel (B) each line plots the evolution over time of the survival probability for each cohort. Sample period: five-year periods from 1955 to 2020, where ‘1955’ corresponds to the period 1951-1955, and ‘2020’ corresponds to the period 2016-2019.

## 4 Calibration & Simulation Method

This section describes our approach to calibrating and simulating the model. For ease of exposition, we first describe our simulation method for a given set of parameter values, before turning to the selection of those parameters. Further details are provided in Appendix B.

### 4.1 Recursive Simulation Method

Let  $x_t$  denote the vector of all endogenous variables in the model in each period  $t$ , and  $d_t$  the vector of (exogenous) drivers as before. The model described in Section 2 can be

written as a function,  $f$ , such that:

$$f(x_{t-1}, x_t, x_{t+1}; d_t) = 0 \quad t = 1, \dots, \infty. \quad (1)$$

Our objective is to explore the role of the drivers,  $d$ , in determining the behavior of one of the elements of  $x$ , namely the equilibrium real interest rate.

As described in Section 3, we have estimates for the drivers over the sample 1955 – 2020, which we will denote by  $t = 1, \dots, H$ . We can input these paths into the model (1), to compute the equilibrium sequence  $\{x_t\}_{t=1}^H$ . However, to do so, we must make an assumption about agents’ expectations of future values of the drivers.

Most of the existing literature studying the secular trend in the equilibrium real interest rate uses an assumption of perfect foresight. In other words, these studies assume that the entire path of  $\{d_t\}_{t=0}^{\infty}$  is known from  $t = 0$ . This is an extreme assumption. The seventy-year sample we consider contains large changes in the drivers over time, as shown in Figures 2 and 3.

Importantly, these changes were not entirely foreseen. Large and persistent forecast errors for demographic variables are documented by, among others, Dowd et al. (2010) and Keilman (1998, 2001). The stock/flow nature of population dynamics implies that forecast errors can cumulate over longer horizons. Indeed, with reference to fifteen-year ahead United Nations cohort population projections, Keilman (1998) notes that forecasts that were “15 or more percent too low for women aged 85+ are not uncommon”.<sup>15</sup> Edge et al. (2007) document persistent forecast errors for long-run productivity growth both in contemporary survey data and earlier academic debates.<sup>16</sup> Jacobs and van Norden (2016) report similar long-run forecast errors in the Federal Reserve’s Greenbook forecasts, linking them to measurement errors in contemporaneous productivity statistics. A number of papers document substantial debate about the prospects for information technology-driven productivity growth in the 1980s and 1990s and the evolution of the corresponding forecasts (see, for example, Stiroh, 2008; Anderson and Kliesen, 2010). Given the close

<sup>15</sup>Note that from the perspective of households within our model such forecasting errors correspond to substantial under-prediction of future survival probabilities.

<sup>16</sup>For example, Perry (1977), Norsworthy et al. (1979) and Denison (2010).

connection between investment-specific technology trends and the relative price of capital, these findings suggest large and persistent forecast errors for the relative price of investment.<sup>17</sup>

In light of this evidence, our simulation method accounts for the gradual updating of beliefs. Specifically, we assume that in each period agents expect the current values of the drivers to prevail forever. This means that they use a random-walk forecasting model:

$$d_{t+i|t} = d_t \quad , \quad i = 0, \dots, \infty .$$

This approach implies that, in each period, the economy is expected to transition to a steady state defined by the values of the drivers in that period. In period  $t$ , the steady state that agents expect the economy to converge to, denoted by  $x_t^{ss}$ , is found by solving:

$$f(x_t^{ss}, x_t^{ss}, x_t^{ss}; d_t) = 0 ,$$

which can be written as an implicit function relating the drivers in any given period to the steady state for the endogenous variables:

$$x_t^{ss} = g(d_t) . \tag{2}$$

Thus, the period  $t$  solution is found by solving for the deterministic transition path to  $x_t^{ss}$ , conditional on  $x_{t-1}$ . The resulting value of  $x_t$  then becomes the initial condition for the subsequent period  $t + 1$  solution.

In this way, the simulation consists of a recursive sequence of projections that account for the evolving information set of agents in the model, consistent with the random-walk forecasting model. Formally, the recursive simulation is constructed as follows:

1. Set an initial condition  $x_0$ .
2. For each period  $t = 1, \dots, H$ , solve (2) to find  $x_t^{ss}$ , i.e., the steady state of the

---

<sup>17</sup>There are fewer investigations of forecast errors for government debt, though [Bachleitner and Pramner \(2023\)](#) find evidence of persistent forecast errors for European economies.

endogenous variables in the model assuming that the drivers stay at their period  $t$  value forever (that is  $d_{t+i} = d_t, i = 1, 2, \dots$ ).

3. For period  $t = 1$ , solve the full deterministic transition path from  $x_0$  to  $x_1^{ss}$  using the dynamic model, (1), under the assumption that  $d_{1+i} = d_1$  for  $i = 1, 2, \dots$ . Record the period 1 solution of this transition path as  $x_1$ .
4. For each period  $t = 2, \dots, H$ , solve the full transition path from  $x_{t-1}$  to  $x_t^{ss}$  using the dynamic model, (1), under the assumption that  $d_{t+i} = d_t$  for  $i = 1, 2, \dots$ . Record the solution for the first period of this transition as  $x_t$ , which will then also become the initial condition for period  $t + 1$ .

The rest of this section describes how the parameters are set and how the initial condition  $x_0$  is chosen.

## 4.2 Calibration of Parameters

We set values for a subset of parameters based on values used in previous studies, as shown in Table 1. In particular, the values for  $\alpha$ ,  $\sigma$ ,  $\delta$  and  $\theta$  follow Lisack et al. (2021) and references therein. The mark-up parameter is set to 0.1, broadly in line with the global estimates for 1980 (roughly the middle of our sample period) presented by De Loecker and Eeckhout (2018). The capital return spread,  $\phi$ , is consistent with an average 2.7% annual spread between the return on capital and the safe real rate.<sup>18</sup>

**Table 1** Baseline parameter values

Parameter	Description	Value
$\alpha$	Weight of capital in production function	0.33
$\sigma$	Elasticity of substitution in production function	0.70
$\delta$	Capital depreciation rate	0.21
$\theta$	Intertemporal elasticity of substitution	1.00
$\mu$	Firms' price mark-up	0.10
$\phi$	Capital return spread	0.22

<sup>18</sup>The average annual spread is estimated by taking the difference between the average product of capital from Caballero et al. (2017) and the long-term real interest rate in Del Negro et al. (2019) using US data.

One of the key model parameters is the vector  $\{\tilde{\beta}_\tau\}_{\tau=1}^T$ , which captures the degree of patience of households at each age. A common approach in models with infinitely-lived agents is to calibrate the (single) discount factor to set the steady-state real interest rate. As we are modeling dynamic changes in the real interest rate, this approach is not directly applicable. Instead, in a similar spirit, we choose these parameters to match two targets in the 1955 steady state ( $x_1^{ss}$ ).

The first target is the real interest rate in the 1955 steady state, which we match to the average of an empirical estimate of Global  $R^*$  over the period 1900–1950. We obtain this estimate using a VAR with common trends using data for the same 31 countries that were used to estimate the drivers (see Section 5.2 below for further details).

The second target is the distribution of asset holdings across households,  $\{a_\tau\}_{\tau=1}^T$ . Evidence on the life-cycle distribution of wealth in Lisack et al. (2021) and Auclert et al. (2021) suggests that, on average, households build up wealth in the early part of life, reach a high-wealth state in middle age, and only partially dissave in old age. To match this pattern, we calibrate the patience parameters such that agents are relatively less patient in middle age and more patient in old age. Appendix B.2 provides further details.

The remaining parameters in the model are the cohort-specific labor supply,  $\{\rho_\tau\}_{\tau=1}^T$ , and the parameters that govern the distribution of monopolistic profits, bequests and taxes among the cohorts. For the latter, we assume that in all cases these are distributed equally among cohorts below age 65 only. In other words we assume  $\mathbf{p}_\tau = \mathbf{b}_\tau = \mathbf{t}_\tau = 1/9$  for  $\tau = 1, \dots, 9$  and  $\mathbf{p}_\tau = \mathbf{b}_\tau = \mathbf{t}_\tau = 0$  for  $\tau = 10, \dots, 14$ . We calibrate  $\rho_\tau$  in line with the evidence on the life-cycle profile of labor-force participation, which is high throughout youth and middle age, starts to fall from around age 65, and is close to zero for the oldest cohorts. Appendix B.2 shows the profile used in the simulations.

Full details of all data used in the calibration are provided in Appendix C.2.

### 4.3 Initial Conditions

The first step in the recursive simulation laid out above is to choose values for the initial conditions,  $x_0$ , which corresponds to 1946-1950. For this, we use data wherever possible.

Importantly, our model and simulation approach allows for a degree of freedom when setting the initial level of the real interest rate ( $r_0$ ). For our simulations, we set the initial interest rate to the average of the empirical estimate of Global  $R^*$  (detailed in Section 5.2) over the corresponding five-year period. This means that the *level* of Global  $R^*$  in our simulations is ‘anchored’ to this initial value, while the structural model and the dynamics of the drivers determine the *change* in Global  $R^*$ .

Where data is not directly available we combine steady-state model relationships with other data to impute consistent values for the missing variables. The full approach is described in detail in Appendix B.3.

## 5 Results

This section presents the results from the model simulation approach described above. We first compare our recursive simulation with a simulation based on ‘perfect foresight’, demonstrating the impact of the assumptions about the evolution of expectations of the drivers. We then compare the model simulation with an empirical estimate from a version of the Del Negro et al. (2019) model using our expanded data set. Finally, we present a decomposition of our simulation to uncover the importance of each driver in determining the path of Global  $R^*$ .

As noted above, each time period in the model lasts for five years, so that the one-period interest rate in the model is a five-year rate of return. For ease of exposition, all interest rates are presented as annualized (i.e., annual equivalent) percentages.<sup>19</sup>

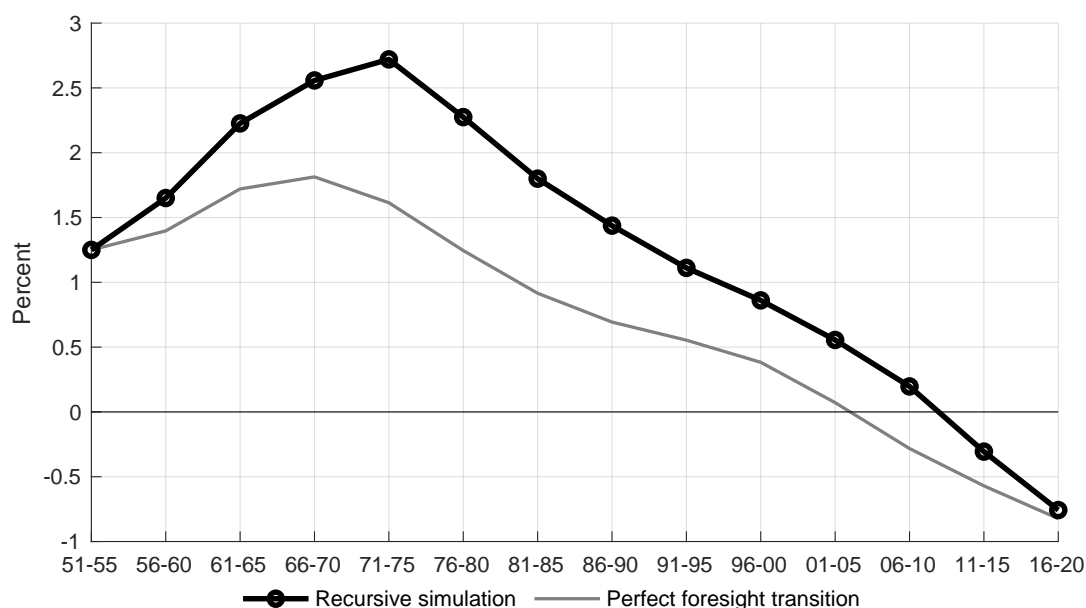
---

<sup>19</sup>The five-year real interest rate in the model is  $r$ , and the annualized equivalent is  $100 \times \left( (1+r)^{\frac{1}{5}} - 1 \right)$ .

## 5.1 Recursive Simulation Results and Properties

Figure 4 presents our baseline recursive simulation alongside a simulation based on the more standard assumption of perfect foresight. The perfect-foresight variant assumes that agents fully anticipate the future paths of all of the drivers from the start of the simulation. The two lines start from the same initial level by construction, and thereafter follow different paths because of the agents' different expectations.

**Figure 4** Global  $R^*$ : Recursive simulation versus perfect foresight transition



NOTE. The black line with circles is the baseline simulation generated by our recursive simulation method. The gray line is the result of a simulation in which the full paths of all drivers are fully anticipated at the start of the simulation. All interest rates are expressed as annualized percentage rates, corresponding to the five-year real interest rates for the periods indicated by x-axis labels.

Our recursive simulation implies that Global  $R^*$  rises from the mid-1950s to the mid-1970s before declining steadily until the end of our sample in 2020. In contrast, when the paths of the drivers are fully anticipated (gray line), the peak in Global  $R^*$  is smaller and occurs earlier. Assuming that agents have perfect foresight implies that they observe the evolution of the drivers until the latter part of our sample (i.e., 2016–2020) at the very start of the simulation (1951–1955). The value of the drivers in the distant future exerts a downward force on equilibrium real interest rates in the early part of the sample because agents foresee the forces that will eventually drive the economy to a steady state

in which the real interest rate will be very low.<sup>20</sup>

In light of the evidence of large and persistent long-term forecast errors discussed in Section 4, we regard the assumptions underpinning the recursive approach in our baseline simulation as more plausible than the assumption that agents foresaw the entire evolution of the drivers from the mid-1950s.

Figure 4 also reveals that both the baseline recursive simulation and the perfect foresight variant imply that Global  $R^*$  drops below zero towards the end of the sample, reaching  $-0.75\%$  in the final period of the simulation. We note that the presence of imperfectly-competitive producers in our model allows the equilibrium real interest rate to be negative, even in the long run (see the discussion in Eggertsson et al., 2019).<sup>21</sup>

Figure 5 sheds further light on the importance of agents' gradual updating of their beliefs, by plotting the full results of each simulation within the recursion alongside the final estimate. In particular, the gray lines show the transition towards steady state, which is constructed in each period using the steps described in Section 4.1. The black line is the baseline estimate, formed by taking the sequence of solutions for the first period of each recursive simulation.

The figure reveals that revisions to the expected paths of the drivers initially led to expectations of persistent increases in Global  $R^*$ , though the subsequent evolution of the drivers pushed up Global  $R^*$  by more than initially expected. That is, in the early part of the simulation, the sequence of recursive paths (gray lines) moved upwards over time. From the mid-1970s, when the baseline estimate of Global  $R^*$  peaks, the expected paths of real rates moved persistently downwards. So from this point on, movements in the drivers led to a sequence of downward revisions in beliefs about the future prospects for Global  $R^*$ .<sup>22</sup>

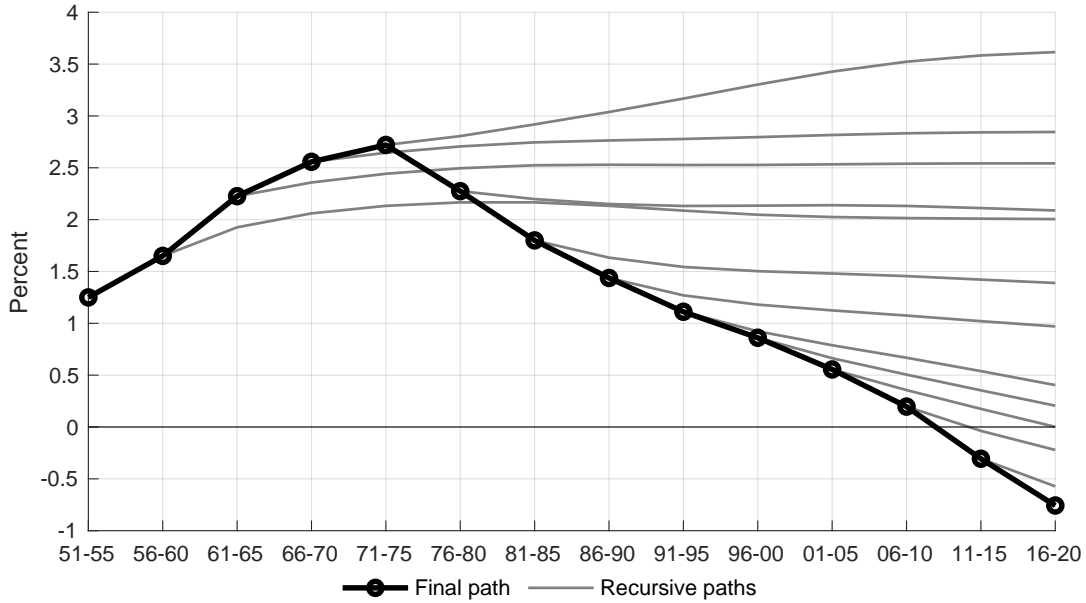
---

<sup>20</sup>We discuss these forces in detail in Section 5.3 below.

<sup>21</sup>As noted in Section 4.3, the level of Global  $R^*$  depends on the initialization of the simulations.

<sup>22</sup>As Figure 5 suggests, beyond 2020 the simulated path of Global  $R^*$  falls further as the world economy continues to adjust to the steady state consistent with 2016-2020 beliefs about the long-run paths of the drivers.

**Figure 5** Global  $R^*$ : Recursive simulation paths



NOTE. The black line with circles is the baseline estimate formed by taking the first period of each recursive simulation, and the gray lines show the sequence of transitions towards steady state from each recursive simulation. All interest rates are expressed as annualized percentage rates, corresponding to the five-year real interest rates for the periods indicated by x-axis labels.

## 5.2 Comparison with an Empirical Estimate

In this section, we compare the simulated path for Global  $R^*$  from the structural model with an empirical estimate of the global trend in real interest rates. As discussed above, the empirical estimate is also used to provide an anchor for the model simulation. In particular, as described in Sections 4.2 and 4.3, we calibrate the initial steady state to be consistent with the historical average of the series, and also set the initial condition for the recursive simulation in line with the empirical estimate.

To derive this empirical estimate, we use a VAR with common trends, closely following the approach of Del Negro et al. (2019), to model the joint dynamics of short-term interest rates, long-term interest rates, and inflation, using annual data from 1900 to 2019.<sup>23</sup> The key innovation is to estimate the model using data from our panel of 31 economies.<sup>24</sup> The

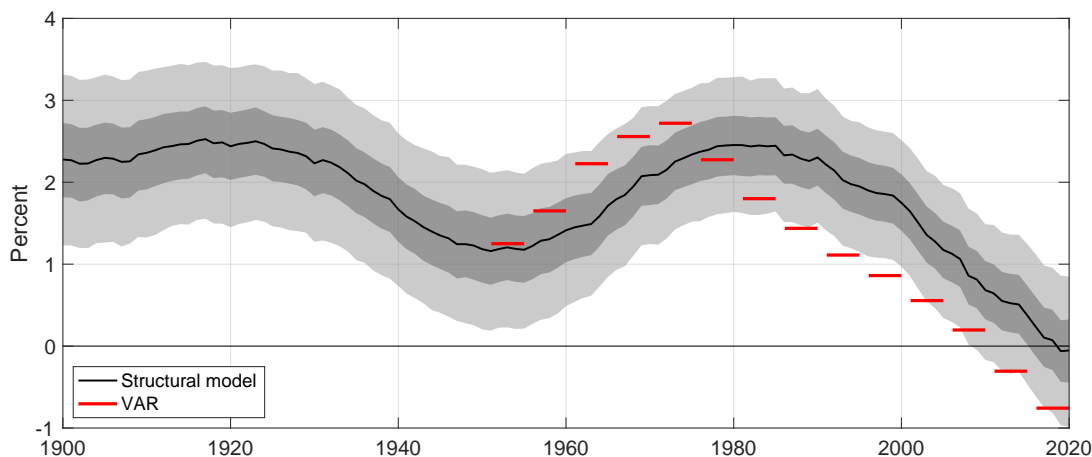
<sup>23</sup>Alternative approaches for the estimation of  $R^*$  include Laubach and Williams (2003), Holston et al. (2017), Lubik and Matthes (2015), Kiley (2020), Ferreira and Shousha (2021), Gonzalez-Astudillo and Laforte (2020) among others.

<sup>24</sup>Figure C.3 in the Appendix reports the raw series for the short-term real interest rates for each country, computed as the nominal short-term interest rate minus the realized inflation rate.

model is cast in state-space form and estimated with Bayesian methods. The details of the model (including the general representation, derivation of the baseline specification, priors, and initial conditions) are reported in Appendix D.

Figure 6 shows the baseline model simulation alongside the VAR estimate. We plot the model simulation as five-year lines, to emphasize that the model determines the interest rate for successive five-year periods, though (as in all other figures) these results are shown as an annualized percentage rate. The VAR estimate of Global  $R^*$  was relatively stable at around 2.25% in the first part of the sample, between 1900 and 1930. After falling to 1.25% around the second world war, the VAR estimate rose again between 1950 and 1980, reaching a peak of around 2.5%. Since the 1980s, the VAR estimate of Global  $R^*$  has been on a downward path, reaching 0% in recent years.<sup>25</sup>

**Figure 6** Baseline model simulation and VAR estimate of Global  $R^*$



NOTE. The solid black line is the posterior median of the VAR estimate of Global  $R^*$  presented in Appendix D and the shaded areas show the 68 and 95 percent posterior intervals. The red lines show the baseline path for the real interest rate generated by the structural model, as shown in Figure 4. All interest rates are annualized percentage rates.

As described in Section 4.3, our initialization approach implies that, by construction, the model simulation and VAR estimates are very close at the start of the simulation. Thereafter the simulated path rises more quickly than the median VAR estimate, peaking slightly earlier. The peak real rate of around 2.5% for 1971–1975 is broadly in line with the

<sup>25</sup>Despite the different approaches and samples of countries, alternative empirical estimates of Global  $R^*$  from the recent literature show similar patterns, especially since the 1980s. See Hamilton et al. (2016), Holston et al. (2017), Glick (2020), Jorda and Taylor (2019), Del Negro et al. (2019) and Kiley (2020).

VAR estimate at that time, lying slightly above the 68% posterior interval. Beyond the peak, the real rate from the model simulation falls more quickly than the VAR estimate and lies towards the bottom of the 95% posterior interval at the end of the sample. Despite these differences in the level, the simulated *change* in Global  $R^*$  from the early 1980s onward, a period that has attracted considerable interest in the literature, is almost identical to our empirical estimate.<sup>26</sup>

### 5.3 Decomposing the Drivers of Global $R^*$

We now turn to the decomposition of the baseline path for Global  $R^*$  into the contributions of individual drivers. Figure 7 shows the baseline simulation, and the decomposition, relative to the 1951–1955 steady-state interest rate.<sup>27</sup>

The estimated decline in Global  $R^*$  from its peak has been primarily driven by changes in longevity and productivity growth. Slower trend productivity growth lowers the rate of return in the economy, reducing Global  $R^*$ . Increased longevity, due to rising survival probabilities in particular for over-65s, raises the stocks of wealth that households wish to hold to fund their retirements. These higher desired wealth holdings have in turn reduced Global  $R^*$ .<sup>28</sup> This finding that demographic factors and productivity growth account for the bulk of the decline in the equilibrium real interest rate are consistent with the results of Eggertsson et al. (2019) for the United States.

Population growth pushes up slightly on Global  $R^*$  throughout the simulation. This is due to the gradual impact of the higher population growth rates in the early part of our sample, ie the ‘baby boom’ generations, which act to raise the working-age population until these generations start reaching retirement in the mid 2010s. As discussed in more

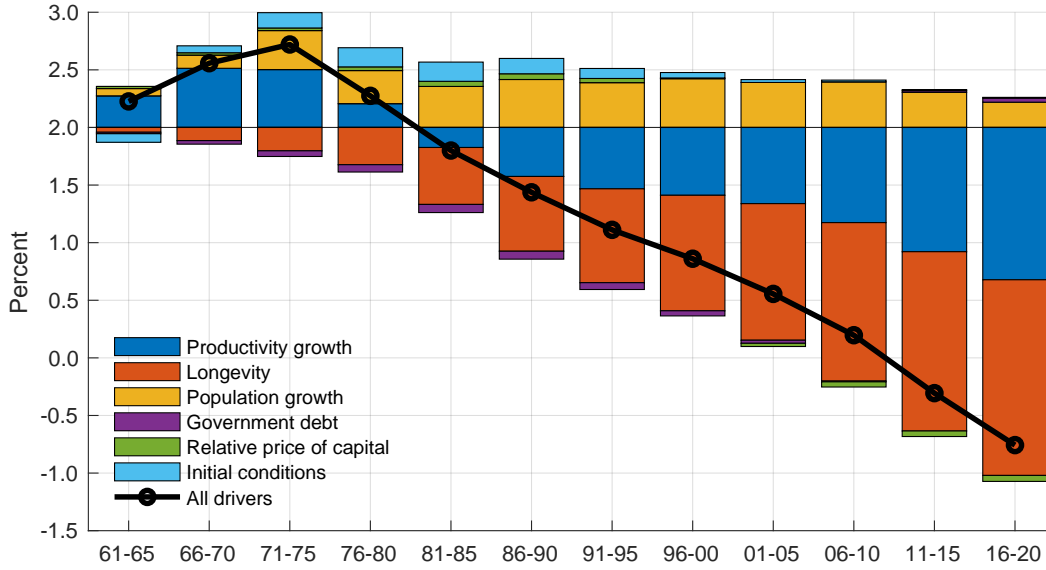
---

<sup>26</sup>As highlighted in Section 4.3, the level of the simulated path of Global  $R^*$  depends on the initialization, while the change between particular dates is less sensitive.

<sup>27</sup>That is, the steady-state real interest rate implied by using the 1951–1955 values of the drivers in equation (2), which is an element of  $x_1^{ss}$ , as described in Section 4.1. Figure 7 is plotted from 1961–1965 onward because this is the first period in which changes in the drivers can affect the real interest rate (as the safe real rate in the model is a pre-determined variable). Specifically, the real interest rate in 1951–1955 is fixed at the value used to initialize the model (i.e., it is an element of  $x_0$ ) and so the level in 1956–1960 reflects the adjustment of the real interest rate towards the steady state implied by the 1951–1955 values of the drivers. Since the figure is plotted relative to the 1951–1955 steady state, the only contribution for 1956–1960 is from ‘initial conditions’ and is therefore omitted.

<sup>28</sup>See Lisack et al. (2021) for more detailed discussion of this mechanism.

**Figure 7** Decomposition of the drivers of Global  $R^*$



NOTE. The black line with circles shows the baseline path from the recursive simulations. Each bar shows the contribution of an individual driver, computed by constructing a simulation in which only that driver changes over the sample (with all other drivers held fixed at their initial values). The light blue bars for the Initial conditions account for the hypothetical transition from  $x_0$  to  $x_1^{ss}$  as defined in Section 4.1. The decomposition is computed relative to the initial steady-state real interest rate, which is set to 2% as described in Section 4.3.

detail in Lisack et al. (2021), this means that the ageing of the population in this period is driven by the significant rise in longevity, rather than the decline in population growth rates since the baby boom, and this is reflected in their impact on Global  $R^*$ . Our finding about the relative importance of longevity, rather than population growth, is also in line with the mechanisms highlighted in Carvalho et al. (2016), and supported by the empirical evidence in Carvalho et al. (2023).

Also in line with other studies (e.g., Sajedi and Thwaites, 2016), the relative price of capital has only a modest effect on the equilibrium real interest rate.

Finally, at a global level, according to the calibration of our model, trend movements in government debt are not sufficient to have a material impact on Global  $R^*$ . In contrast, the model used in Eggertsson et al. (2019) suggests that higher government debt raised the interest rate in the US substantially from 1970 to 2015. This difference is due to both the larger rise in debt in the US, with a doubling over this period in their simulations, and calibration differences between our models, such as a higher inter-temporal substitution,

which makes demand for assets less elastic in their model.<sup>29</sup>

Our simulation does not include the effects of several other potential drivers of real interest rates. In Appendix E we draw on existing literature to discuss the likely implications of these additional drivers. To the extent that mark-ups, risk and inequality have been increasing over time, we would expect these factors to exert downward pressure on Global  $R^*$ . Rising retirement ages and greater provision of health and social insurance could in principle work in the opposite direction.

## 5.4 Sensitivity to Parameter Values and Drivers

We now examine the sensitivity of the structural model simulation of Global  $R^*$  to alternative assumptions about key simulation inputs, namely the values of model parameters and the paths of the drivers.

To do so, we re-compute the simulation under alternative assumptions about the values of key parameters and the paths of the drivers. We consider alternative values for the elasticity of intertemporal substitution ( $\theta$ ), the production-function elasticity ( $\sigma$ ), and the group of cohort-specific parameters governing the life-cycle distribution of labor supply, bequests, taxes and monopolistic profits from producers ( $\{\rho_\tau, \mathbf{b}_\tau, \mathbf{t}_\tau, \xi_\tau\}_{\tau=1}^T$ ). For the drivers, we consider alternative values for the smoothing parameter in the HP filter used for the relative price of capital, government debt to GDP and productivity growth. For each parameter or driver, we specify a discrete set of two alternative assumptions, which, alongside the baseline assumption, gives a set of three possible values for each. We draw random combinations from the total set of alternative assumptions and re-run the recursive simulations for each draw.<sup>30</sup> Appendix B.4 provides further details of this exercise.

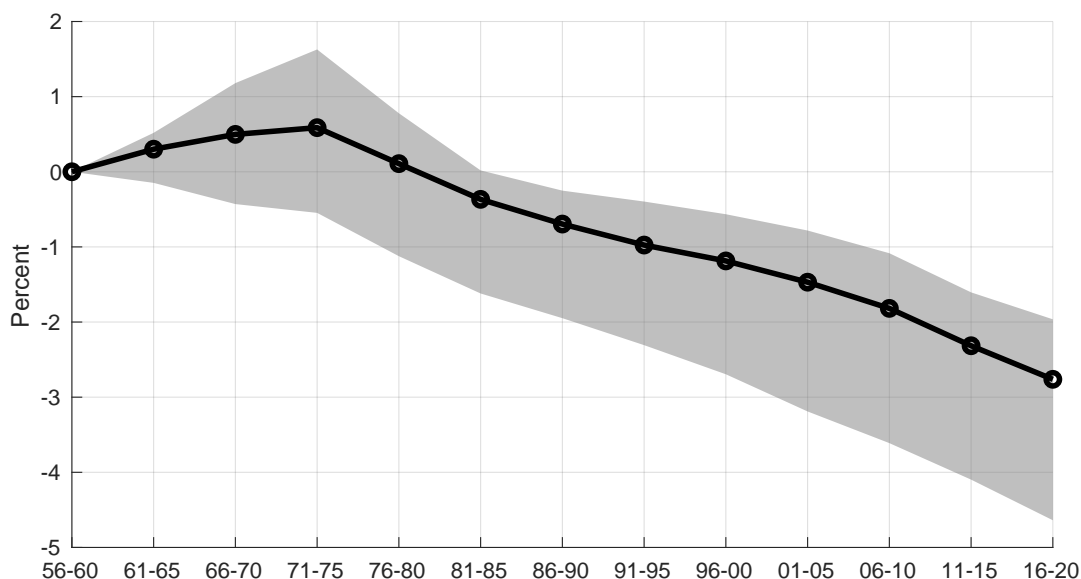
Figure 8 summarizes the results of this experiment. We focus on the effects of the drivers on Global  $R^*$ , computed as the sum of the decomposition bars shown in Figure 7,

---

<sup>29</sup>We include these parameters in the sensitivity checks in the next section.

<sup>30</sup>Although there are only three alternatives for each parameter/driver, we allow a large number of parameters and drivers to vary, such that the total number of possible combinations is around 40,000. Given the computational overhead of the recursive simulation method, we assess sensitivity using a random sample of 1,000 combinations.

**Figure 8** Sensitivity of the effects of drivers on Global  $R^*$



NOTE. The black line with circles shows the effects of the drivers in the baseline simulations, relative to the initial steady state. The gray swathe is the range (minimum to maximum) of simulations from 1,000 random draws of alternative assumptions for model parameters and the paths of the drivers. Appendix B.4 provides full details. The units are annual percentage points.

excluding the contribution from initial conditions, relative to the 1951-1955 steady state. Examining the results in this form allows us to focus on the effects of the drivers on Global  $R^*$ , abstracting from the effects of alternative assumptions on the initial steady state and the transitional dynamics from the initial conditions. It therefore permits a ‘like-for-like’ assessment of how the effects of the drivers on Global  $R^*$  vary under alternative assumptions. The solid black line plots the effects of the drivers for our baseline assumptions, and the gray swathe plots the full range – minimum to maximum – of the results obtained drawing from the alternative assumptions.

Figure 8 shows that plausible alternative assumptions generate a wide range of estimates of the effects of the drivers on Global  $R^*$ . For the set of alternatives we consider, the range of estimates spans around 2.5 percentage points in 2020, though the range is skewed to the downside of our baseline estimate. Overall, the steady decline in Global  $R^*$  since the early 1970s is a robust feature of simulations under a range of plausible alternative parameter values.

## 6 Conclusion

This paper has explored the behavior and determinants of the global trend real interest rate – Global  $R^*$  – from 1950 to 2020 using a rich data set to calibrate and simulate a structural model of the world economy, accounting for slow-moving beliefs about long-term trends. Simulations of the model imply that Global  $R^*$  increased from the mid-1950s to the mid-1970s before steadily declining. This decline is driven by falling productivity growth and increased longevity, while other drivers have smaller, and partially offsetting, effects.

By identifying the main drivers of past movements in Global  $R^*$ , our findings can also inform the debate about its long-run prospects. For example, without a significant reversal in the long-run trends in productivity growth and population aging, Global  $R^*$  is likely to remain persistently low. Such an outlook could create challenges and opportunities for the design and implementation of macroeconomic policy frameworks (Blanchard, 2019; Bailey et al., 2022; Grimm et al., 2023). While our model can also be used to produce forecasts for Global  $R^*$ , doing so reliably requires forecasting the underlying drivers themselves, as well as judgments about new drivers that may emerge. These questions represent important avenues for future research.

## References

- ADJEMIAN, S., H. BASTANI, M. JUILLARD, F. MIHOUBI, G. PERENDIA, M. RATTO, AND S. VILLEMOT (2011): “Dynare: Reference manual, version 4,” .
- ALVAREDO, F., L. CHANCEL, T. PIKETTY, E. SAEZ, AND G. ZUCMAN (2017): “Global Inequality Dynamics: New Findings from WID.world,” *American Economic Review*, 107, 404–409.
- ANDERSON, R. G. AND K. L. KLIESEN (2010): “FOMC learning and productivity growth (1985–2003): A reading of the record,” *Federal Reserve Bank of St. Louis Review*, 129–154.
- AUCLERT, A., H. MALMBERG, F. MARTENET, AND M. ROGNLIE (2021): “Demographics, Wealth, and Global Imbalances in the Twenty-First Century,” Working Paper 29161, National Bureau of Economic Research.
- AUCLERT, A. AND M. ROGNLIE (2017): “Aggregate Demand and the Top 1 Percent,” *American Economic Review Papers & Proceedings*, 107, 588–92.
- (2018): “Inequality and Aggregate Demand,” Working Paper 24280, National Bureau of Economic Research.
- BACHLEITNER, A. AND D. PRAMMER (2023): “Don’t Blame the Government!? An Assessment of Debt Forecast Errors with a View to the Economic Governance Review,” *mimeo*.
- BAILEY, A. (2022): “The Economic Landscape: Structural Change, Global  $R^*$ , and the Missing Investment Puzzle,” *Speech at the Official Monetary and Financial Institutions Forum, 12 July*.
- BAILEY, A., A. CESA-BIANCHI, M. GAROFALO, R. HARRISON, N. MCLAREN, S. PITON, AND R. SAJEDI (2022): “Structural Change, Global  $R^*$ , and the Missing Investment Puzzle,” *Supporting paper for Bailey (2022)*.
- BLANCHARD, O. (2019): “Public Debt and Low Interest Rates,” *American Economic Review*, 109, 1197–1229.
- BORDO, M. D., B. EICHENGREEN, AND J. KIM (1998): “Was there really an earlier period of international financial integration comparable to today?” *NBER Working Paper*.
- CABALLERO, R. J., E. FARHI, AND P.-O. GOURINCHAS (2017): “Rents, Technical Change, and Risk Premia Accounting for Secular Trends in Interest Rates, Returns on Capital, Earning Yields, and Factor Shares,” *American Economic Review*, 107, 614–20.
- CARVALHO, C., A. FERRERO, F. MEZIN, AND F. NECHIO (2023): “Demographics and Real Interest Rates Across Countries and Time,” *mimeo*.
- CARVALHO, C., A. FERRERO, AND F. NECHIO (2016): “Demographics and real interest rates: Inspecting the mechanism,” *European Economic Review*, 88, 208–226.
- CHINN, M. D. AND H. ITO (2006): “What matters for financial development? Capital controls, institutions, and interactions,” *Journal of Development Economics*, 81, 163–192.
- (2008): “A new measure of financial openness,” *Journal of Comparative Policy Analysis*, 10, 309–322.

- DAVIS, J., C. FUENZALIDA, L. HUETSCH, B. MILLS, AND A. M. TAYLOR (2023): “Global Natural Rates in the Long Run: Postwar Macro Trends and the Market-Implied  $r^*$  in 10 Advanced Economies,” Nber international seminar on macroeconomics, National Bureau of Economic Research, Inc.
- DE LOECKER, J. AND J. EECKHOUT (2018): “Global Market Power,” Working Paper 24768, National Bureau of Economic Research.
- DE LOECKER, J., J. EECKHOUT, AND G. UNGER (2020): “The Rise of Market Power and the Macroeconomic Implications,” *The Quarterly Journal of Economics*, 135, 561–644.
- DEL NEGRO, M., D. GIANNONE, M. P. GIANNONI, AND A. TAMBALOTTI (2017): “Safety, Liquidity, and the Natural Rate of Interest,” *Brookings Papers on Economic Activity*, 48, 235–316.
- (2019): “Global trends in interest rates,” *Journal of International Economics*, 118, 248–262.
- DENISON, E. F. (2010): *Accounting for slower economic growth: the United States in the 1970’s*, Brookings Institution Press.
- DIEZ, F. J., D. LEIGH, AND S. TAMBUNLERTCHAI (2018): “Global Market Power and its Macroeconomic Implications,” IMF Working Papers 2018/137, International Monetary Fund.
- DOWD, K., D. BLAKE, AND A. J. CAIRNS (2010): “Facing up to uncertain life expectancy: The longevity fan charts,” *Demography*, 47, 67–78.
- EDGE, R. M., T. LAUBACH, AND J. C. WILLIAMS (2007): “Learning and shifts in long-run productivity growth,” *Journal of Monetary Economics*, 54, 2421–2438.
- EGGERTSSON, G. B., N. R. MEHROTRA, AND J. A. ROBBINS (2019): “A model of secular stagnation: Theory and quantitative evaluation,” *American Economic Journal: Macroeconomics*, 11, 1–48.
- FARHI, E. AND F. GOURIO (2018): “Accounting for Macro-Finance Trends: Market Power, Intangibles, and Risk Premia,” *Brookings Papers on Economic Activity*, 49, 147–250.
- FERREIRA, T. R. T. AND S. SHOUSA (2021): “Supply of Sovereign Safe Assets and Global Interest Rates,” International Finance Discussion Papers 1315, Board of Governors of the Federal Reserve System (U.S.).
- GIANNONE, D., M. LENZA, AND G. E. PRIMICERI (2015): “Prior Selection for Vector Autoregressions,” *The Review of Economics and Statistics*, 97, 436–451.
- GLICK, R. (2020): “ $r^*$  and the global economy,” *Journal of International Money and Finance*, 102.
- GONZALEZ-ASTUDILLO, M. P. AND J.-P. LAFORTE (2020): “Estimates of  $r^*$  Consistent with a Supply-Side Structure and a Monetary Policy Rule for the U.S. Economy,” Finance and Economics Discussion Series 2020-085, Board of Governors of the Federal Reserve System (U.S.).
- GOURINCHAS, P.-O., H. REY, AND M. SAUZET (2022): “Global Real Rates: A Secular Approach,” CEPR Discussion Papers 16941, C.E.P.R. Discussion Papers.

- GRIMM, M., O. JORDÀ, M. SCHULARICK, AND A. M. TAYLOR (2023): “Loose Monetary Policy and Financial Instability,” NBER Working Papers 30958, National Bureau of Economic Research, Inc.
- HAMILTON, J. D., E. S. HARRIS, J. HATZIUS, AND K. D. WEST (2016): “The Equilibrium Real Funds Rate: Past, Present, and Future,” *IMF Economic Review*, 64, 660–707.
- HOLSTON, K., T. LAUBACH, AND J. C. WILLIAMS (2017): “Measuring the natural rate of interest: International trends and determinants,” *Journal of International Economics*, 108, 59–75.
- JACOBS, J. P. AND S. VAN NORDEN (2016): “Why are initial estimates of productivity growth so unreliable?” *Journal of Macroeconomics*, 47, 200–213.
- JORDA, O., M. SCHULARICK, AND A. M. TAYLOR (2017): “Macrofinancial History and the New Business Cycle Facts,” *NBER Macroeconomics Annual*, 31, 213–263.
- JORDA, O. AND A. M. TAYLOR (2019): “Riders on the Storm,” NBER Working Papers 26262, National Bureau of Economic Research.
- KEILMAN, N. (1998): “How accurate are the United Nations world population projections?” *Population and Development Review*, 24, 15–41.
- (2001): “Data quality and accuracy of United Nations population projections, 1950-95,” *Population Studies*, 55, 149–164.
- KILEY, M. T. (2020): “The Global Equilibrium Real Interest Rate: Concepts, Estimates, and Challenges,” *Annual Review of Financial Economics*, 12, 305–326.
- LAUBACH, T. AND J. C. WILLIAMS (2003): “Measuring the Natural Rate of Interest,” *The Review of Economics and Statistics*, 85, 1063–1070.
- LISACK, N., R. SAJEDI, AND G. THWAITES (2017): “Demographic trends and the real interest rate,” *Bank of England Staff Working Paper No. 701*.
- (2021): “Population Ageing and the Macroeconomy,” *International Journal of Central Banking*, 17, 43–80.
- LUBIK, T. A. AND C. MATTHES (2015): “Calculating the Natural Rate of Interest: A Comparison of Two Alternative Approaches,” *Richmond Fed Economic Brief*.
- MARX, M., B. MOJON, AND F. R. VELDE (2021): “Why have interest rates fallen far below the return on capital?” *Journal of Monetary Economics*, 124, 57–76.
- MIAN, A., L. STRAUB, AND A. SUFI (2021): “What explains the decline in  $r^*$ ? Rising income inequality versus demographic shifts,” *Proceedings of the 2021 Jackson Hole Symposium*.
- MOLL, B., L. RACHEL, AND P. RESTREPO (2021): “Uneven growth: automation’s impact on income and wealth inequality,” Bank of England working papers 913, Bank of England.
- MORENO BADIA, M. M., S. MBAYE, AND K. CHAE (2018): “Global Debt Database: Methodology and Sources,” IMF Working Papers 2018/111, International Monetary Fund.

- NORSWORTHY, J. R., M. J. HARPER, AND K. KUNZE (1979): “The Slowdown in Productivity Growth: Analysis of Some Contributing Factors,” *Brookings Papers on Economic Activity*, 1979, 387–421.
- OBSTFELD, M. (2023): “Natural and Neutral Real Interest Rates: Past and Future,” Asian Monetary Policy Forum Commissioned Paper, ABFER.
- OECD (2021): “Pensions at a glance,” *OECD and G20 Indicators*.
- PERRY, G. L. (1977): “Potential Output and Productivity,” *Brookings Papers on Economic Activity*, 1977, 11–60.
- PESARAN, M. H. (2006): “Estimation and Inference in Large Heterogeneous Panels with a Multifactor Error Structure,” *Econometrica*, 74, 967–1012.
- PLATZER, J. AND M. PERUFFO (2022): “Secular Drivers of the Natural Rate of Interest in the United States: A Quantitative Evaluation,” IMF working papers, International Monetary Fund.
- RACHEL, L. AND T. D. SMITH (2017): “Are Low Real Interest Rates Here to Stay?” *International Journal of Central Banking*, 13, 1–42.
- RACHEL, L. AND L. H. SUMMERS (2019): “On falling neutral real rates, fiscal policy and the risk of secular stagnation,” in *Brookings Papers on Economic Activity*, vol. 7.
- SAJEDI, R. AND G. THWAITES (2016): “Why are Real Interest Rates So Low? The Role of the Relative Price of Investment Goods,” *IMF Economic Review*, 64, 635–659.
- STIROH, K. (2008): “Information technology and productivity: Old answers and new questions,” *CEifo Economic Studies*, 54, 358–385.
- ZIESEMER, T. (2021): “Labour-augmenting technical change data for alternative elasticities of substitution: growth, slowdown, and distribution dynamics,” *Economics of Innovation and New Technology*, 1–27.

# Appendix

## A Theoretical Framework: Derivations

### A.1 Full Model

The timing convention is such that a subscript  $t$  means the variable is determined (known) in period  $t$ , and for assets this means the end-of-period quantity. For simplicity, in most places we leave as implicit the expectations operator for future variables.

#### Household Optimization

We consider overlapping generations of households, with the age of each household indexed by  $\tau = 1, \dots, T$ . Households face probabilistic mortality:  $\Pi_{t,\tau}$  will denote the probability that a household that was aged  $(\tau - 1)$  in period  $(t - 1)$  will survive for one more period, to reach age  $\tau$  in period  $t$ . Note that  $\Pi_{t,1} = 1$  and  $\Pi_{t,T+1} = 0$  for all  $t$ .

Each period, households maximize utility from consumption subject to their budget constraint. They have access to an asset,  $a$ , which pays a net real interest rate,  $r$ . At each age households supply  $\rho_\tau$  units of labor inelastically and earn a wage per effective units of labor,  $w$ .

Specifically, in period  $t$ , a household aged  $\tau$ , with existing assets  $a_{t-1,\tau-1}$  brought forward from the previous period, will solve the following recursive maximization problem:

$$\max_{c_{t,\tau}, a_{t,\tau}} V(t, \tau, a_{t-1,\tau-1}) = \beta_\tau \frac{c_{t,\tau}^{1-\theta}}{1-\theta} + \mathbb{E}_t \left[ \Pi_{t+1,\tau+1} V(t+1, \tau+1, a_{t,\tau}) \right],$$

subject to:

$$c_{t,\tau} + a_{t,\tau} = \rho_\tau w_t + (1 + r_{t-1})a_{t-1,\tau-1} + \varpi_{t,\tau}, \quad (\text{A.1})$$

where  $\beta_\tau$  is an age-specific utility weight and  $\varpi_{t,\tau}$  is age-specific non-labor income, which the households take as exogenous, and which will be defined below.

We assume that households are born with no assets, and do not have any incentives to retain assets when  $\tau = T$ , so that  $a_{t,0} = a_{t,T} = 0$  for all  $t$ .

This optimization leads to a set of  $(T - 1)$  Euler equations:

$$c_{t,\tau}^{-\theta} = \frac{\beta_{\tau+1}}{\beta_\tau} \mathbb{E}_t \left[ \Pi_{t+1,\tau+1} (1 + r_t) c_{t+1,\tau+1}^{-\theta} \right] \quad \text{for } \tau = 1, \dots, T - 1.$$

We introduce the notation  $\tilde{\beta}_\tau \equiv \beta_{\tau+1}/\beta_\tau$ , denoting the relative weights on utility at age  $\tau+1$  and  $\tau$ . In this way,  $\tilde{\beta}_\tau$  corresponds to the more familiar notion of the household's 'patience'

at age  $\tau$ . As such, we can rewrite the Euler equations as:

$$c_{t,\tau}^{-\theta} = \tilde{\beta}_\tau \mathbb{E}_t \left[ \Pi_{t+1,\tau+1} (1+r_t) c_{t+1,\tau+1}^{-\theta} \right] \quad \text{for } \tau = 1, \dots, T-1. \quad (\text{A.2})$$

Thus the household's problem is defined in terms of the  $(2T-1)$  choice variables  $\{c_{t,\tau}\}_{\tau=1\dots T}$  and  $\{a_{t,\tau}\}_{\tau=1\dots T-1}$ , the  $(T-1)$  Euler equations, and the  $T$  budget constraints.

## Firms

A monopolistic retailer buys an intermediate good and sells it with a net mark-up,  $\mu$ , over its marginal cost. Normalizing the price of the final good to 1, this means the relative price of the intermediate good is given by  $1/(1+\mu)$ . The aggregate profit of the retailer, given by:

$$\mathcal{P}_t = Y_t \mu / (1 + \mu) \quad (\text{A.3})$$

is distributed to the households. The intermediate good is produced using a CES aggregation of capital, brought forward from the previous period, and effective units of labor:

$$Y_t = \left( \alpha K_{t-1}^{\frac{\sigma-1}{\sigma}} + (1-\alpha)(E_t L_t)^{\frac{\sigma-1}{\sigma}} \right)^{\frac{\sigma}{\sigma-1}} \quad (\text{A.4})$$

where  $E_t$  is a labor-augmenting technological process with net growth rate  $e_t$ .

The intermediate-good-producing firm's profit maximization can be written as:

$$\max_{K_t, L_t} \frac{1}{(1+\mu)} Y_t - (r_t^k p_t^k K_{t-1} + w_t L_t)$$

where  $p^k$  is the relative price of capital,  $r^k$  is the rental rate of capital, and  $w$  is the wage per units of labor. This gives the first-order conditions:

$$r_t^k = \frac{1}{(1+\mu)} \alpha \frac{1}{p_t^k} \left( \frac{Y_t}{K_{t-1}} \right)^{\frac{1}{\sigma}} \quad (\text{A.5})$$

$$w_t = \frac{1}{(1+\mu)} (1-\alpha) E_t^{\frac{\sigma-1}{\sigma}} \left( \frac{Y_t}{L_t} \right)^{\frac{1}{\sigma}} \quad (\text{A.6})$$

## Government

The government has a stock of debt,  $G$ , on which it pays interest,  $r$ . This interest payment is financed by lump-sum taxes levied on households,  $\mathcal{T}$ . Hence their budget constraint is given by:

$$G_t = (1 + r_{t-1})G_{t-1} - \mathcal{T}_t$$

This can be written in ratio to output:

$$\frac{G_t}{Y_t} = (1 + r_{t-1})\frac{G_{t-1}}{Y_t} - \frac{\mathcal{T}_t}{Y_t} \quad (\text{A.7})$$

## Financial Intermediary

At the end of each period, a financial intermediary takes the aggregate assets of the households, promising a net return of  $r_t$  per unit in the next period. They turn these assets, net of government bonds, into the capital good, with a technology that transforms 1 unit of the consumption good into  $p_t^k$  units of capital goods. The intermediary stores these capital goods and makes them available for production in the next period. As above,  $K_t$  denotes the capital stock available for production in period  $t + 1$ . Hence the financial intermediary must repay  $(1 + r_t)p_t^k K_t$  to the households in period  $t + 1$ .

To pay this return, the intermediary rents the capital stock to the firm. The firm pays the rental cost,  $r_{t+1}^k K_t$ , and returns the un-depreciated capital stock,  $(1 - \delta)K_t$ , to the intermediary. Furthermore, if the relative price of capital goods changes, the intermediary earns this revenue at relative price  $p_{t+1}^k$ . Hence the profit of the intermediary, denominated in terms of the consumption goods, is:

$$\begin{aligned} \Phi_{t+1} &= p_{t+1}^k \left( r_{t+1}^k K_t + (1 - \delta)K_t \right) - (1 + r_t)p_t^k K_t \\ &= \left( (1 + r_{t+1}^k - \delta) \frac{p_{t+1}^k}{p_t^k} - (1 + r_t) \right) p_t^k K_t \\ &= \phi p_t^k K_t, \end{aligned}$$

where we have denoted by  $\phi$  the profit per unit of capital, which we assume to be fixed. In other words,  $\phi$  represents a fixed spread between the return on capital and the risk-free rate:

$$1 + r_t = (1 + r_{t+1}^k - \delta) \frac{p_{t+1}^k}{p_t^k} - \phi.$$

These profits are treated as a resource cost to the economy, which can also be viewed as an additional cost that the financial intermediary is paying, such as the cost of storing capital.

## Aggregation and Market Clearing

**Population Growth** Let  $N_{t,\tau}$  be the size of the cohort aged  $\tau$  at time  $t$ . The law of motion of cohort sizes is given by:

$$N_{t,\tau} = \Pi_{t,\tau} N_{t-1,\tau-1} \quad \text{for } \tau = 2, \dots, T. \quad (\text{A.8})$$

We denote the net growth rate of consecutive cohorts entering the model as:

$$n_t \equiv \frac{N_{t,1} - N_{t-1,1}}{N_{t-1,1}}.$$

We will refer to this as the “population growth rate”, but note that this is not the fertility or birth rate, nor the aggregate population growth rate, except in steady state.

**Labor** Total labor supply is given by:

$$L_t = \sum_{\tau=1}^T N_{t,\tau} \rho_{\tau} \quad (\text{A.9})$$

**Asset markets** The aggregate assets of the household are either used to buy the stock of government bonds, or turned into capital by the financial intermediary:

$$p_t^k K_t + G_t = \sum_{\tau=1}^T N_{t,\tau} a_{t,\tau} \quad (\text{A.10})$$

The households that die between periods leave their assets, along with the return, as accidental bequests. We can define aggregate accidental bequests as:

$$\mathcal{B}_t = (1 + r_{t-1}) \sum_{\tau=1}^T (1 - \Pi_{t,\tau+1}) N_{t-1,\tau} a_{t-1,\tau} \quad (\text{A.11})$$

**Goods markets** Define aggregate consumption:

$$C_t = \sum_{\tau=1}^T N_{t,\tau} c_{t,\tau} \quad (\text{A.12})$$

We can sum up the budget constraints of all the households alive in a given period:

$$\begin{aligned} C_t &= w_t \sum_{\tau=1}^T N_{t,\tau} \rho_{\tau} - \sum_{\tau=1}^T N_{t,\tau} a_{t,\tau} + (1 + r_{t-1}) \sum_{\tau=1}^T N_{t,\tau} a_{t-1,\tau-1} + \sum_{\tau=1}^T N_{t,\tau} \varpi_{t,\tau} \\ &= L_t w_t - p_t^k K_t - G_t + (1 + r_{t-1}) \sum_{\tau=1}^T N_{t,\tau} a_{t-1,\tau-1} + \sum_{\tau=1}^T N_{t,\tau} \varpi_{t,\tau} \end{aligned}$$

The non-labor income of the household,  $\varpi$ , comprises of the monopolistic profit of the retailer and the accidental bequests, minus the lump-sum taxes paid to the government. Since we have defined these objects as aggregates in each period, we need to distribute them among

the different generations:

$$N_{t,\tau}\varpi_{t,\tau} = \mathbf{p}_\tau \mathcal{P}_t + \mathbf{b}_\tau \mathcal{B}_t - \mathbf{t}_\tau \mathcal{T}_t \quad (\text{A.13})$$

with  $\sum_{\tau=1}^T \mathbf{p}_\tau = \sum_{\tau=1}^T \mathbf{b}_\tau = \sum_{\tau=1}^T \mathbf{t}_\tau = 1$ .

Plugging this into the aggregate budget constraint above we have:

$$C_t = L_t w_t - p_t^k K_t - G_t + (1 + r_{t-1}) \sum_{\tau=1}^T N_{t,\tau} a_{t-1,\tau-1} + \mathcal{P}_t + \mathcal{B}_t - \mathcal{T}_t$$

Bringing in the government budget constraint, we have:

$$\begin{aligned} C_t &= L_t w_t - p_t^k K_t - G_t + (1 + r_{t-1}) \sum_{\tau=1}^T N_{t,\tau} a_{t-1,\tau-1} + \mathcal{P}_t + \mathcal{B}_t + G_t - (1 + r_{t-1}) G_{t-1} \\ &= L_t w_t - p_t^k K_t + (1 + r_{t-1}) \sum_{\tau=1}^T N_{t,\tau} a_{t-1,\tau-1} + \mathcal{P}_t + \mathcal{B}_t - (1 + r_{t-1}) G_{t-1} \end{aligned}$$

Bringing in the definition of aggregate bequests, we have:

$$\begin{aligned} C_t &= L_t w_t - p_t^k K_t + (1 + r_{t-1}) \sum_{\tau=1}^T N_{t,\tau} a_{t-1,\tau-1} + \mathcal{P}_t + (1 + r_{t-1}) \sum_{\tau=1}^T (1 - \Pi_{t,\tau+1}) N_{t-1,\tau} a_{t-1,\tau} \\ &\quad - (1 + r_{t-1}) G_{t-1} \\ &= L_t w_t - p_t^k K_t + (1 + r_{t-1}) \sum_{\tau=1}^T N_{t,\tau} a_{t-1,\tau-1} + (1 + r_{t-1}) \sum_{\tau=1}^T (1 - \Pi_{t,\tau+1}) N_{t-1,\tau} a_{t-1,\tau} \\ &\quad + \mathcal{P}_t - (1 + r_{t-1}) G_{t-1} \\ &= L_t w_t - p_t^k K_t + (1 + r_{t-1}) \sum_{\tau=0}^{T-1} N_{t,\tau+1} a_{t-1,\tau} + (1 + r_{t-1}) \sum_{\tau=1}^T (1 - \Pi_{t,\tau+1}) N_{t-1,\tau} a_{t-1,\tau} \\ &\quad + \mathcal{P}_t - (1 + r_{t-1}) G_{t-1} \\ &= L_t w_t - p_t^k K_t + (1 + r_{t-1}) \sum_{\tau=1}^T N_{t,\tau+1} a_{t-1,\tau} + (1 + r_{t-1}) \sum_{\tau=1}^T (1 - \Pi_{t,\tau+1}) N_{t-1,\tau} a_{t-1,\tau} \\ &\quad + \mathcal{P}_t - (1 + r_{t-1}) G_{t-1} \end{aligned}$$

where the final line follows from the fact that  $N_{t,T+1} = 0$ , and  $a_{t,0} = 0$  for all  $t$ . Bringing terms together, we have:

$$\begin{aligned} C_t &= L_t w_t - p_t^k K_t + (1 + r_{t-1}) \sum_{\tau=1}^T \{N_{t,\tau+1} + (1 - \Pi_{t,\tau+1}) N_{t-1,\tau}\} a_{t-1,\tau} + \mathcal{P}_t - (1 + r_{t-1}) G_{t-1} \\ &= L_t w_t - p_t^k K_t + (1 + r_{t-1}) \sum_{\tau=1}^T \{\Pi_{t,\tau+1} N_{t-1,\tau} + (1 - \Pi_{t,\tau+1}) N_{t-1,\tau}\} a_{t-1,\tau} + \mathcal{P}_t - (1 + r_{t-1}) G_{t-1} \\ &= L_t w_t - p_t^k K_t + (1 + r_{t-1}) \sum_{\tau=1}^T N_{t-1,\tau} a_{t-1,\tau} + \mathcal{P}_t - (1 + r_{t-1}) G_{t-1} \end{aligned}$$

where the second equation used the law of motion of the cohort sizes shown above.

Bringing in the period  $(t - 1)$  asset market clearing condition, we have:

$$\begin{aligned}
C_t &= L_t w_t - p_t^k K_t + (1 + r_{t-1}) \left( p_{t-1}^k K_{t-1} + G_{t-1} \right) + \mathcal{P}_t - (1 + r_{t-1}) G_{t-1} \\
&= L_t w_t - p_t^k K_t + (1 + r_{t-1}) \left( p_{t-1}^k K_{t-1} \right) + \mathcal{P}_t \\
&= L_t w_t + (1 + r_{t-1}) p_{t-1}^k K_{t-1} - p_t^k K_t + \mathcal{P}_t
\end{aligned}$$

First consider the terms involving capital:

$$\begin{aligned}
(1 + r_{t-1}) p_{t-1}^k K_{t-1} - p_t^k K_t &= \left( (1 + r_t^k - \delta) \frac{p_t^k}{p_{t-1}^k} - \phi \right) p_{t-1}^k K_{t-1} - p_t^k K_t \\
&= (1 + r_t^k - \delta) p_t^k K_{t-1} - \phi p_{t-1}^k K_{t-1} - p_t^k K_t \\
&= r_t^k p_t^k K_{t-1} + (1 - \delta) p_t^k K_{t-1} - p_t^k K_t - \phi p_{t-1}^k K_{t-1} \\
&= r_t^k p_t^k K_{t-1} - p_t^k (K_t - (1 - \delta) K_{t-1}) - \phi p_{t-1}^k K_{t-1} \\
&= r_t^k p_t^k K_{t-1} - p_t^k I_t - \Phi_t
\end{aligned}$$

where we have defined investment as  $I_t = K_t - (1 - \delta) K_{t-1}$ . Plugging this back in to the above:

$$C_t = L_t w_t + r_t^k p_t^k K_{t-1} - p_t^k I_t - \Phi_t + \mathcal{P}_t$$

Rearranging:

$$C_t + p_t^k I_t + \Phi_t = L_t w_t + r_t^k p_t^k K_{t-1} + \mathcal{P}_t$$

The zero-profit condition of the intermediate goods producer implies:

$$L_t w_t + r_t^k p_t^k K_{t-1} = \frac{1}{1 + \mu} Y_t$$

and using the definition of the profit of the retailer, we can write the right hand side of the above as:

$$L_t w_t + r_t^k p_t^k K_{t-1} + \mathcal{P}_t = \frac{1}{1 + \mu} Y_t + \frac{\mu}{1 + \mu} Y_t = Y_t$$

Plugging this in, we have the aggregate resource constraint:

$$Y_t = C_t + p_t^k I_t + \Phi_t$$

This says that all goods produced must either be consumed, invested or earned as profit by the financial intermediary.

## Exogenous Processes

The exogenous processes in the model are described by random walks:

$$n_t = n_{t-1} + \epsilon_t^n \quad (\text{A.14})$$

$$\Pi_{t,\tau} = \Pi_{t-1,\tau} + \epsilon_t^{\Pi_\tau} \quad \text{for } \tau = 2, \dots, T \quad (\text{A.15})$$

$$e_t = e_{t-1} + \epsilon_t^e \quad (\text{A.16})$$

$$\frac{G_t}{Y_t} = \frac{G_{t-1}}{Y_{t-1}} + \epsilon_t^G \quad (\text{A.17})$$

$$p_t^k = p_{t-1}^k + \epsilon_t^{pk} \quad (\text{A.18})$$

## A.2 Stationarizing the Model

The model has two sources of growth in steady state: technological growth at rate  $e_t$  and population growth at rate  $n_t$ . Our objective is to write the equations of the model in terms of only stationary variables, taking into account these two sources of steady-state growth.

We first define the size of each cohort as a share of the total labor supply:

$$n_{t,\tau} \equiv \frac{N_{t,\tau}}{L_t}$$

with which we can re-write the law of motion of the cohort sizes as:

$$\begin{aligned} n_{t,\tau} &= \frac{N_{t,\tau}}{L_t} = \frac{\Pi_{t,\tau} N_{t-1,\tau-1} L_{t-1}}{L_{t-1} L_t} \\ &= \Pi_{t,\tau} n_{t-1,\tau-1} (1 + l_t)^{-1} \quad \tau = 2, \dots, T \end{aligned} \quad (\text{A.19})$$

where we have defined the net growth rate of total labor supply:

$$l_t \equiv \frac{L_t - L_{t-1}}{L_{t-1}}$$

For  $n_{t,1}$ , we have:

$$\begin{aligned} n_{t,1} &= \frac{N_{t,1}}{L_t} = \frac{(1 + n_t) N_{t-1,1} L_{t-1}}{L_{t-1} L_t} \\ &= n_{t-1,1} \frac{1 + n_t}{1 + l_t} \end{aligned} \quad (\text{A.20})$$

The preceding equations show how we can determine the population shares in terms of recursive equations which depend on ex-post mortality rates and total labor force growth.

Using the definition of the total labor supply:

$$1 + l_t = \frac{L_t}{L_{t-1}} = \frac{\sum_{\tau=1}^T \rho_{\tau} N_{t,\tau}}{L_{t-1}}$$

which we can write as:

$$1 + l_t = \sum_{\tau=1}^T \rho_{\tau} m_{t,\tau} \quad (\text{A.21})$$

where we have defined an auxiliary variable:

$$m_{t,\tau} \equiv \frac{N_{t,\tau}}{L_{t-1}}$$

which is the size of each cohort relative to the size of the *previous period's* working population.<sup>31</sup>

Following the same steps as for  $n_{t,\tau}$ , we can express  $m_{t,\tau}$  recursively:

$$\begin{aligned} m_{t,\tau} &= \frac{N_{t,\tau}}{L_{t-1}} = \frac{\Pi_{t,\tau} N_{t-1,\tau-1} L_{t-2}}{L_{t-2} L_{t-1}} \\ &= \Pi_{t,\tau} m_{t-1,\tau-1} (1 + l_{t-1})^{-1} \quad \tau = 2, \dots, T \end{aligned} \quad (\text{A.22})$$

and:

$$m_{t,1} = \frac{1 + n_t}{1 + l_{t-1}} m_{t-1,1} \quad (\text{A.23})$$

We can write the production function per effective units of labor:

$$\frac{Y_t}{E_t L_t} = \left( \alpha \left( \frac{K_{t-1}}{E_t L_t} \right)^{\frac{\sigma-1}{\sigma}} + (1 - \alpha) \right)^{\frac{\sigma}{\sigma-1}}$$

For aggregate variables, we use lower cases to denote them per effective units of labor, i.e.

---

<sup>31</sup>To compute the steady-state values of  $m$  note that:

$$m_{t,\tau} = \frac{N_{t,\tau}}{L_t} \frac{L_t}{L_{t-1}} = n_{t,\tau} (1 + l_t)$$

so in steady state, we have:

$$m_{\tau} = (1 + l) n_{\tau} \quad \tau = 1, \dots, T$$

$z_t = Z_t/E_t L_t$ , so that:

$$\begin{aligned}
k_{t-1} &= \frac{K_{t-1}}{E_{t-1}L_{t-1}} \\
&= \frac{K_{t-1}}{E_t L_t} \frac{E_t L_t}{E_{t-1} L_{t-1}} \\
&= \frac{K_{t-1}}{E_t L_t} \frac{E_t}{E_{t-1}} \frac{L_t}{L_{t-1}} \\
&= \frac{K_{t-1}}{E_t L_t} (1 + e_t)(1 + l_t)
\end{aligned}$$

This means we can write:

$$y_t = \left( \alpha \left( \frac{k_{t-1}}{(1 + e_t)(1 + l_t)} \right)^{\frac{\sigma-1}{\sigma}} + (1 - \alpha) \right)^{\frac{\sigma}{\sigma-1}} \quad (\text{A.24})$$

The factor prices can be written:

$$r_t^k = \frac{1}{(1 + \mu)} \alpha \frac{1}{p_t^k} \left( \frac{(1 + e_t)(1 + l_t)y_t}{k_{t-1}} \right)^{\frac{1}{\sigma}} \quad (\text{A.25})$$

$$\tilde{w}_t = \frac{1}{(1 + \mu)} (1 - \alpha) (y_t)^{\frac{1}{\sigma}} \quad (\text{A.26})$$

Where we define  $\tilde{w}_t \equiv w_t/E_t$ , since the wage was already defined per units of labor.

We can also redefine the total profits per unit of effective labor:

$$\tilde{\mathcal{P}}_t \equiv \frac{\mathcal{P}_t}{E_t L_t} = \frac{\mu}{(1 + \mu)} y_t \quad (\text{A.27})$$

We can redefine the costs from the capital spread in the same way:

$$\tilde{\Phi}_t = \phi p_{t-1}^k k_{t-1} / (1 + e_t)(1 + l_t) \quad (\text{A.28})$$

and the aggregate bequests:

$$\begin{aligned}
\tilde{\mathcal{B}}_t &= (1 + r_{t-1}) \sum_{\tau=1}^T (1 - \Pi_{t,\tau+1}) \frac{N_{t-1,\tau}}{E_t L_t} a_{t-1,\tau} \\
&= (1 + r_{t-1}) \sum_{\tau=1}^T (1 - \Pi_{t,\tau+1}) \frac{N_{t-1,\tau}}{E_{t-1} L_{t-1}} a_{t-1,\tau} \frac{E_{t-1} L_{t-1}}{E_t L_t} \\
&= (1 + r_{t-1}) \sum_{\tau=1}^T (1 - \Pi_{t,\tau+1}) \frac{N_{t-1,\tau}}{L_{t-1}} \frac{a_{t-1,\tau}}{E_{t-1}} \frac{E_{t-1} L_{t-1}}{E_t L_t} \\
&= (1 + r_{t-1}) \sum_{\tau=1}^T (1 - \Pi_{t,\tau+1}) n_{t-1,\tau} \tilde{a}_{t-1,\tau} \frac{E_{t-1} L_{t-1}}{E_t L_t} \\
&= \frac{(1 + r_{t-1})}{(1 + e_t)(1 + l_t)} \sum_{\tau=1}^T (1 - \Pi_{t,\tau+1}) n_{t-1,\tau} \tilde{a}_{t-1,\tau}
\end{aligned} \tag{A.29}$$

where we defined  $\tilde{a}_{t,\tau} \equiv a_{t,\tau}/E_t$ , as  $a_{t,\tau}$  are already in per-capita terms.

We can also rewrite the period  $t$  Euler equations (now dropping the expectations operator for simplicity):

$$\begin{aligned}
1 &= \tilde{\beta}_\tau \Pi_{t+1,\tau+1} \left( \frac{c_{t+1,\tau+1}}{c_{t,\tau}} \right)^{-\theta} (1 + r_t) \\
&= \tilde{\beta}_\tau \Pi_{t+1,\tau+1} \left( \frac{c_{t+1,\tau+1}}{E_{t+1}} \frac{E_t}{c_{t,\tau}} \frac{E_{t+1}}{E_t} \right)^{-\theta} (1 + r_t) \\
&= \tilde{\beta}_\tau \Pi_{t+1,\tau+1} \left( \frac{\tilde{c}_{t+1,\tau+1}}{\tilde{c}_{t,\tau}} (1 + e_{t+1}) \right)^{-\theta} (1 + r_t) \\
&= \tilde{\beta}_\tau \Pi_{t+1,\tau+1} \left( \frac{\tilde{c}_{t+1,\tau+1}}{\tilde{c}_{t,\tau}} \right)^{-\theta} (1 + e_{t+1})^{-\theta} (1 + r_t) \quad \text{for } \tau = 1, \dots, T-1
\end{aligned} \tag{A.30}$$

where we defined  $\tilde{c}_{t,\tau} \equiv c_{t,\tau}/E_t$ .

Similarly, the aggregate consumption can be written:

$$\begin{aligned}
c_t &= \sum_{\tau=1}^T \frac{N_{t,\tau}}{L_t} \frac{c_{t,\tau}}{E_t} \\
&= \sum_{\tau=1}^T n_{t,\tau} \tilde{c}_{t,\tau}
\end{aligned} \tag{A.31}$$

The non-labor income can be written:

$$\begin{aligned}
\varpi_{t,\tau} &= \frac{1}{N_{t,\tau}} (\mathbf{p}_\tau \mathcal{P}_t + \mathbf{b}_\tau \mathcal{B}_t - \mathbf{t}_{t,\tau} \mathcal{T}_t) \\
&= \frac{E_t L_t}{N_{t,\tau}} (\mathbf{p}_\tau \tilde{\mathcal{P}}_t + \mathbf{b}_\tau \tilde{\mathcal{B}}_t - \mathbf{t}_{t,\tau} \tilde{\mathcal{T}}_t) \\
&= \frac{E_t}{n_{t,\tau}} (\mathbf{p}_\tau \tilde{\mathcal{P}}_t + \mathbf{b}_\tau \tilde{\mathcal{B}}_t - \mathbf{t}_{t,\tau} \tilde{\mathcal{T}}_t) \\
n_{t,\tau} \tilde{\varpi}_{t,\tau} &= \mathbf{p}_\tau \tilde{\mathcal{P}}_t + \mathbf{b}_\tau \tilde{\mathcal{B}}_t - \mathbf{t}_{t,\tau} \tilde{\mathcal{T}}_t
\end{aligned} \tag{A.32}$$

where we defined  $\tilde{\varpi}_{t,\tau} \equiv \varpi_{t,\tau}/E_t$ .

The budget constraints can be written as:

$$\begin{aligned}
\tilde{c}_{t,\tau} &= \rho_{t,\tau} \tilde{w}_t + (1 + r_{t-1}) \tilde{a}_{t-1,\tau-1} \frac{E_{t-1}}{E_t} - \tilde{a}_{t,\tau} + \tilde{\varpi}_{t,\tau} \\
&= \rho_{t,\tau} \tilde{w}_t + \frac{(1 + r_{t-1})}{(1 + e_t)} \tilde{a}_{t-1,\tau-1} - \tilde{a}_{t,\tau} + \tilde{\varpi}_{t,\tau} \quad \text{for } \tau = 1, \dots, T
\end{aligned} \tag{A.33}$$

The capital spread definition remains unchanged:

$$(1 + r_t) = (1 + r_{t+1}^k - \delta) \frac{p_{t+1}^k}{p_t^k} - \phi \tag{A.34}$$

The asset market clearing condition can be written:

$$p_t^k k_t + g_t = \sum_{\tau=1}^T n_{t,\tau} \tilde{a}_{t,\tau} \tag{A.35}$$

Writing the government budget constraint in ratio to total output:

$$\begin{aligned}
\frac{G_t}{Y_t} &= (1 + r_{t-1}) \frac{G_{t-1}}{Y_{t-1}} \frac{Y_{t-1}}{Y_t} - \frac{\mathcal{T}_t}{Y_t} \\
\frac{g_t}{y_t} &= (1 + r_{t-1}) \frac{g_{t-1}}{y_{t-1}} \frac{y_{t-1}}{y_t} \frac{E_{t-1} L_{t-1}}{E_t L_t} - \frac{\tilde{\mathcal{T}}_t}{y_t} \\
&= (1 + r_{t-1}) \frac{g_{t-1}}{y_{t-1}} \frac{y_{t-1}/y_t}{(1 + e_t)(1 + l_t)} - \frac{\tilde{\mathcal{T}}_t}{y_t}
\end{aligned} \tag{A.36}$$

The exogenous processes remain unchanged:

$$n_t = n_{t-1} + \epsilon_t^n \quad (\text{A.37})$$

$$\Pi_{t,\tau} = \Pi_{t-1,\tau} + \epsilon_t^{\Pi_\tau} \quad \text{for } \tau = 2, \dots, T \quad (\text{A.38})$$

$$e_t = e_{t-1} + \epsilon_t^e \quad (\text{A.39})$$

$$\frac{g_t}{y_t} = \frac{g_{t-1}}{y_{t-1}} + \epsilon_t^G \quad (\text{A.40})$$

$$p_t^k = p_{t-1}^k + \epsilon_t^{pk} \quad (\text{A.41})$$

### A.3 Final Model Equations

$$n_{t,\tau} = \Pi_{t,\tau} n_{t-1,\tau-1} (1 + l_t)^{-1} \quad \tau = 2, \dots, T \quad (\text{A.42})$$

$$n_{t,1} = n_{t-1,1} \frac{1 + n_t}{1 + l_t} \quad (\text{A.43})$$

$$1 + l_t = \sum_{\tau=1}^T \rho_\tau m_{t,\tau} \quad (\text{A.44})$$

$$m_{t,\tau} = \Pi_{t,\tau} m_{t-1,\tau-1} (1 + l_{t-1})^{-1} \quad \tau = 2, \dots, T \quad (\text{A.45})$$

$$m_{t,1} = \frac{1 + n_t}{1 + l_{t-1}} m_{t-1,1} \quad (\text{A.46})$$

$$y_t = \left( \alpha \left( \frac{k_{t-1}}{(1 + e_t)(1 + l_t)} \right)^{\frac{\sigma-1}{\sigma}} + (1 - \alpha) \right)^{\frac{\sigma}{\sigma-1}} \quad (\text{A.47})$$

$$r_t^k = \frac{1}{(1 + \mu)} \alpha \frac{1}{p_t^k} \left( \frac{(1 + e_t)(1 + l_t) y_t}{k_{t-1}} \right)^{\frac{1}{\sigma}} \quad (\text{A.48})$$

$$\tilde{w}_t = \frac{1}{(1 + \mu)} (1 - \alpha) (y_t)^{\frac{1}{\sigma}} \quad (\text{A.49})$$

$$\tilde{p}_t = \frac{\mu}{(1 + \mu)} y_t \quad (\text{A.50})$$

$$\tilde{\Phi}_t = \phi p_{t-1}^k k_{t-1} / (1 + e_t)(1 + l_t) \quad (\text{A.51})$$

$$\tilde{B}_t = \frac{(1 + r_{t-1})}{(1 + e_t)(1 + l_t)} \sum_{\tau=1}^T (1 - \Pi_{t,\tau+1}) n_{t-1,\tau} \tilde{a}_{t-1,\tau} \quad (\text{A.52})$$

$$1 = \tilde{\beta}_\tau \Pi_{t+1,\tau+1} \left( \frac{\tilde{c}_{t+1,\tau+1}}{\tilde{c}_{t,\tau}} \right)^{-\theta} (1 + e_{t+1})^{-\theta} (1 + r_t) \quad \text{for } \tau = 1, \dots, T - 1 \quad (\text{A.53})$$

$$c_t = \sum_{\tau=1}^T n_{t,\tau} \tilde{c}_{t,\tau} \quad (\text{A.54})$$

$$\tilde{c}_{t,\tau} = \rho_\tau \tilde{w}_t + \frac{(1 + r_{t-1})}{(1 + e_t)} \tilde{a}_{t-1,\tau-1} - \tilde{a}_{t,\tau} + \tilde{\omega}_{t,\tau} \quad \text{for } \tau = 1, \dots, T \quad (\text{A.55})$$

$$n_{t,\tau} \tilde{\omega}_{t,\tau} = \mathbf{p}_\tau \tilde{\mathcal{P}}_t + \mathbf{b}_\tau \tilde{\mathcal{B}}_t - \mathbf{t}_{t,\tau} \tilde{\mathcal{T}}_t \quad \text{for } \tau = 1, \dots, T \quad (\text{A.56})$$

$$(1 + r_t) = (1 + r_{t+1}^k - \delta) \frac{p_{t+1}^k}{p_t^k} - \phi \quad (\text{A.57})$$

$$p_t^k k_t + g_t = \sum_{\tau=1}^T n_{t,\tau} \tilde{a}_{t,\tau} \quad (\text{A.58})$$

$$\frac{g_t}{y_t} = (1 + r_{t-1}) \frac{g_{t-1}}{y_{t-1}} \frac{y_{t-1}/y_t}{(1 + e_t)(1 + l_t)} - \frac{\tilde{\mathcal{T}}_t}{y_t} \quad (\text{A.59})$$

$$n_t = n_{t-1} + \epsilon_t^n \quad (\text{A.60})$$

$$\Pi_{t,\tau} = \Pi_{t-1,\tau} + \epsilon_t^{\Pi_\tau} \quad \text{for } \tau = 2, \dots, T \quad (\text{A.61})$$

$$e_t = g_{t-1} + \epsilon_t^e \quad (\text{A.62})$$

$$\frac{g_t}{y_t} = \frac{g_{t-1}}{y_{t-1}} + \epsilon_t^G \quad (\text{A.63})$$

$$p_t^k = p_{t-1}^k + \epsilon_t^{p^k} \quad (\text{A.64})$$

## A.4 Steady-State Equations

$$n_\tau = \Pi_\tau n_{\tau-1} (1 + l)^{-1} \quad \tau = 2, \dots, T \quad (\text{A.65})$$

$$l = n \quad (\text{A.66})$$

$$1 + l = \sum_{\tau=1}^T \rho_\tau m_\tau \quad (\text{A.67})$$

$$m_\tau = (1 + l) n_\tau \quad \text{for } \tau = 1, \dots, T \quad (\text{A.68})$$

$$y = \left( \alpha \left( \frac{k}{(1 + e)(1 + l)} \right)^{\frac{\sigma-1}{\sigma}} + (1 - \alpha) \right)^{\frac{\sigma}{\sigma-1}} \quad (\text{A.69})$$

$$r^k = \frac{1}{(1 + \mu)} \alpha \frac{1}{p^k} \left( \frac{(1 + e)(1 + l)y}{k} \right)^{\frac{1}{\sigma}} \quad (\text{A.70})$$

$$\tilde{w} = \frac{1}{(1 + \mu)} (1 - \alpha) (y)^{\frac{1}{\sigma}} \quad (\text{A.71})$$

$$\tilde{\mathcal{P}} = \frac{\mu}{(1 + \mu)} y \quad (\text{A.72})$$

$$\tilde{\Phi} = \phi p^k k / (1 + e)(1 + l) \quad (\text{A.73})$$

$$\tilde{\mathcal{B}} = \frac{(1 + r)}{(1 + e)(1 + l)} \sum_{\tau=1}^T (1 - \Pi_{\tau+1}) n_\tau \tilde{a}_\tau \quad (\text{A.74})$$

$$1 = \tilde{\beta}_\tau \Pi_{\tau+1} \left( \frac{\tilde{c}_{\tau+1}}{\tilde{c}_\tau} \right)^{-\theta} (1 + e)^{-\theta} (1 + r) \quad \text{for } \tau = 1, \dots, T - 1 \quad (\text{A.75})$$

$$c = \sum_{\tau=1}^T n_{\tau} \tilde{c}_{\tau} \quad (\text{A.76})$$

$$\tilde{c}_{\tau} = \rho_{\tau} \tilde{w} + \frac{(1+r)}{(1+e)} \tilde{a}_{\tau-1} - \tilde{a}_{\tau} + \tilde{\omega}_{\tau} \quad \text{for } \tau = 1, \dots, T \quad (\text{A.77})$$

$$n_{\tau} \tilde{\omega}_{\tau} = \mathbf{p}_{\tau} \tilde{\mathcal{P}} + \mathbf{b}_{\tau} \tilde{\mathcal{B}} - \mathbf{t}_{\tau} \tilde{\mathcal{T}} \quad \text{for } \tau = 1, \dots, T \quad (\text{A.78})$$

$$(1+r) = 1 + r^k - \delta - \phi \quad (\text{A.79})$$

$$p^k k + g = \sum_{\tau=1}^T n_{\tau} \tilde{a}_{\tau} \quad (\text{A.80})$$

$$\left( \frac{(1+r)}{(1+e)(1+l)} - 1 \right) \frac{g}{y} = \frac{\tilde{\mathcal{T}}}{y} \quad (\text{A.81})$$

## B Theoretical Framework: Computational Details

This Appendix provides further details of the recursive simulation approach, the calibration of parameters, the process for setting the initial conditions of the simulation and the exercise to examine sensitivity of the results to alternative assumptions.

### B.1 Recursive simulation method

As noted in the main text, the recursive simulation method amounts to computing a sequence of transition paths to a sequence of steady states that are consistent with a random walk assumption for the drivers. This approach is straightforward to implement in the Dynare package (Adjemian et al., 2011).

### B.2 Calibration

**Discount factors.** We assume that households have different different degrees of patience during three phases of life: ‘young’; ‘middle aged’ and ‘old’:

$$\tilde{\beta}_{\tau} = \begin{cases} \tilde{\beta}_Y & 1 \leq \tau < 5 \\ \tilde{\beta}_M & 5 \leq \tau < 11 \\ \tilde{\beta}_O & 11 \leq \tau \leq 14 \end{cases} \quad (\text{B.1})$$

We choose the parameters  $\tilde{\beta}_Y$ ,  $\tilde{\beta}_M$  and  $\tilde{\beta}_O$  to best match two ‘targets’:

1. The real interest rate in the 1951–1955 steady state is close to the VAR estimate over

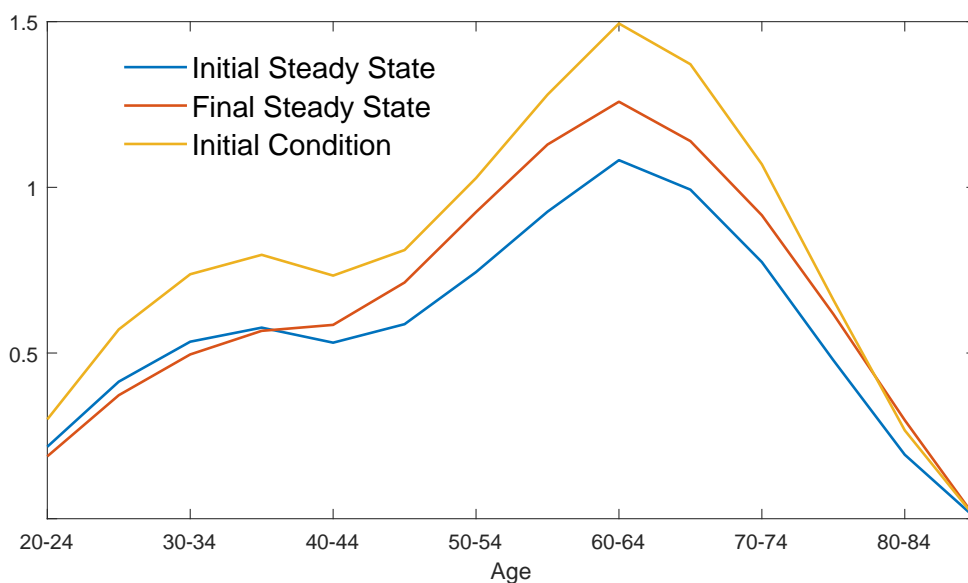
the past (until 1950). Specifically, the target for the 1951–1955 steady-state annual real interest rate is 2% (taken from the pre-1950 average of the VAR estimate, which is 2.04%, rounded to the nearest quarter of a percentage point).

2. The distribution of per capita assets  $\{a_\tau\}_{\tau=1}^T$  matches a stylized distribution based on data on life-cycle asset holdings (see Lisack et al., 2021, for example). Specifically, the target per capita asset levels are 0.5, 1 and 0.75 for young, middle-aged and old households respectively.<sup>32</sup>

This is achieved by numerically minimizing a quadratic distance between the steady-state solution and the target. A weight of 10 is placed on matching the steady-state real interest rate and a weight of 1 is placed on matching the steady-state life-cycle asset distribution.

This process gives values for the discount factors of  $\tilde{\beta}_Y = 1.22$ ,  $\tilde{\beta}_M = 0.88$  and  $\tilde{\beta}_O = 1.72$ , and leads to the life-cycle wealth distribution plotted in Figure B.1.

**Figure B.1** Assets per capita over the life-cycle,  $a_\tau$

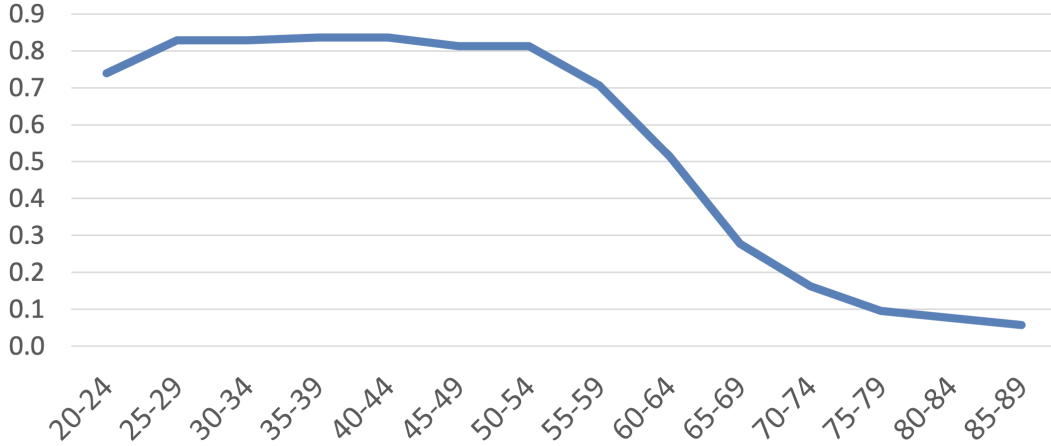


NOTE. Assets per capita at each age group, for the steady states implied by the initial (1951-55) values of all drivers, the final (2015-2019) values of all drivers, and the initial conditions corresponding to 1950, relative to each corresponding GDP.

**Labor supply.** Figure B.2 shows the profile of labor supply over the life-cycle. In the model, this is given by the parameters  $\rho_\tau$ , for  $\tau = 1, \dots, T$ , which corresponds to the age groups from 20-24 to 85-89. The precise calibration is based on US data, where we have sufficient granularity across cohorts, but the evidence is in line with other countries.

<sup>32</sup>We target the normalized levels (i.e., the *relative* sizes of asset holdings across cohorts).

**Figure B.2** Labor supply over the life-cycle,  $\rho_\tau$



NOTE. The figure plots the labor force participation rate by age group for the US, average over the available years (1996, 2006, 2016).

### B.3 Initial conditions

Our recursive simulation approach requires us to set initial conditions that correspond to 1946–1950. In particular, the initial condition for any variable that appears in the model equations with a lag will affect the period 1 solution. The objective is to use data where available and otherwise to use steady-state relationships from the model.

1. Data from 1950 is used to set the initial conditions for  $p_0^k$  and  $GY_0$ .
2. The VAR estimate of the equilibrium real interest rate in 1951–1955 is used to set  $r_0$ . We set  $r_0$  consistent with an annual rate of 1.25%, taken from the 1951–1955 average of the VAR estimate, which is 1.18%, rounded to the nearest quarter of a percentage point.
3. Population data for 1950 is used to directly set the initial conditions for the population shares in each cohort,  $\{n_{0,\tau}\}_{\tau=1}^T$ .
4. The initial population growth rate,  $n_0$ , is set to the first observed value in 1951–1955.
5. Output,  $y_0$ , productivity growth,  $e_0$ , and labor force growth,  $l_0$ , are set equal to their 1951–1955 steady-state values.
6. Adjusted population shares,  $\{m_{0,\tau}\}_{\tau=1}^T$  are set by ‘inverting’ the recursive laws of motion in the model:

$$m_{0,1} = m_{1,1} (1 + l_0) / (1 + n_0)$$

$$m_{0,\tau} = \Pi_{1,\tau+1}^{-1} (1 + l_0) m_{1,\tau+1}, \quad \tau = 2, \dots, T$$

where  $\{m_{1,\tau}\}_{\tau=1}^T$  are the adjusted population shares in 1951–1955 computed directly from the data. Setting the  $\{m_{0,\tau}\}_{\tau=1}^T$  in this way ensures that the initial observed population structure is accurately captured in the simulation.

7. The initial capital stock  $k_0$  is set by combining the capital to output ratio observed in the data with the assumption for initial output  $y_0$  using the relationship:

$$k_0 = s_{ky} \frac{y_0 (1 + l_0) (1 + e_0)}{p_0^k}$$

where  $s_{ky}$  is the capital to output ratio in 1955, computed using the Penn World Table data for our sample of 31 countries.

## B.4 Construction of the ‘sensitivity swathe’ (Figure 8)

We construct Figure 8 by replicating the recursive simulation under alternative assumptions about model parameter values and the paths of some drivers.

For the model parameters, we consider the following sets of values (where the first element is our baseline assumption):

- $\theta \in \{1, 0.90, 1.1\}$
- $\sigma \in \{0.7, 1, 1.1\}$

For the cohort-specific distribution of non-labor income ( $\{\mathbf{b}_\tau, \mathbf{t}_\tau, \mathbf{p}_\tau\}_{\tau=1}^T$ ) we consider two alternative assumptions:

- An equal allocation across all cohorts:  $\mathbf{b}_\tau = \mathbf{t}_\tau = \mathbf{p}_\tau = \frac{1}{T}, \tau = 1, \dots, T$
- A distribution skewed towards older households:  $\mathbf{b}_\tau = \mathbf{t}_\tau = \mathbf{p}_\tau = 0, \tau = 1, \dots, 9$ ;  $\mathbf{b}_\tau = \mathbf{t}_\tau = \mathbf{p}_\tau = 0.2, \tau = 10, \dots, 14$

For the drivers (government debt to GDP, productivity growth, relative price of capital) we use alternative detrending assumptions, by considering two alternative values of  $\lambda$  in the filtering process:  $\lambda = 100$  and  $\lambda = 10,000$ .

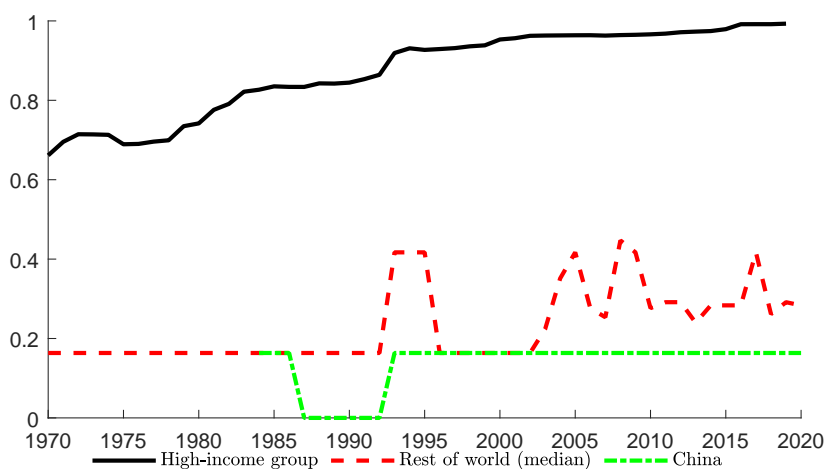
## C Data

**List of countries.** Our sample comprises 31 ‘high-income’ countries. A country is defined as high income if its output per capita in 2014 (computed as expenditure-side real GDP at current PPPs in mil. 2011US\$ divided by total population from PWT9.0) is above 25,000\$. From this list of countries, we remove oil-producing countries and ‘fiscal paradises’.

The final list of countries is: Australia, Austria, Belgium, Canada, Czechia, Denmark, Estonia, Finland, France, Germany, Greece, Hong Kong, Hungary, Iceland, Ireland, Israel, Italy, Japan, Korea, Lithuania, Netherlands, New Zealand, Norway, Poland, Portugal, Singapore, Spain, Sweden, Switzerland, United Kingdom, United States.

A notable exclusion from our group of countries is China. However, despite rapid GDP growth and trade liberalization during the later part of the sample period, China’s financial openness remained relatively low throughout the sample, as shown in Figure C.1. On that basis, we do not consider that including China in our group of countries would satisfy the conditions for the group to be considered as a fully integrated world economy.

**Figure C.1** Capital account openness: ‘high income country’ group and China



*Notes:* The figure shows the GDP-weighted index of capital market openness developed by Chinn and Ito (2006, 2008) for our 31 ‘high income countries’ and the index for China.

### C.1 Structural Model: Drivers

#### Population Growth

*Description:* Total population, both sexes combined, by five-year age groups. The population growth rate of is the growth rate of the size of the cohort aged 20-24 at the end of each five-year period. *Source:* United Nations, Department of Economic and Social Affairs, Population Division (2017).

*Aggregation:* Sum over 31 countries.

*Sample:* 1950-2020.

*Adjustments:* None.

### **Survival Probability**

*Description:* Total population, both sexes combined, by five-year age groups. The probability of survival is calculated by dividing the population of a certain five-year age group at the end of a given five-year period by the previous (younger) five-year age group at the end of the previous five year period. *Source:* United Nations, Department of Economic and Social Affairs, Population Division (2017).

*Aggregation:* Sum over 31 countries.

*Sample:* 1950-2020.

*Adjustments:* Our approach can lead to survival probabilities that are larger than 1, reflecting migration (which can lead to a cohort to be growing in size over time). In these cases, we set the survival probability to 1.

### **Government debt to GDP ratio**

*Description:* General government debt as a percent of GDP. *Source:* [Moreno Badia et al. \(2018\)](#).

*Aggregation:* Cross-sectional weighted average of country-specific data with time-varying GDP weights from PWT (expenditure-side real GDP at current PPPs, in mil. 2017US\$).

*Sample:* 1950-2017.

### **Labor-augmenting productivity**

*Description:* Labor-augmenting technical change data derived from a CES production function using data from Penn World Table 9.1. *Source:* [Ziesemer \(2021\)](#).

*Aggregation:* Cross-sectional weighted average of country-specific data with time-varying GDP weights from PWT (expenditure-side real GDP at current PPPs, in mil. 2017US\$).

*Sample:* 1950-2017.

### **Relative price of capital**

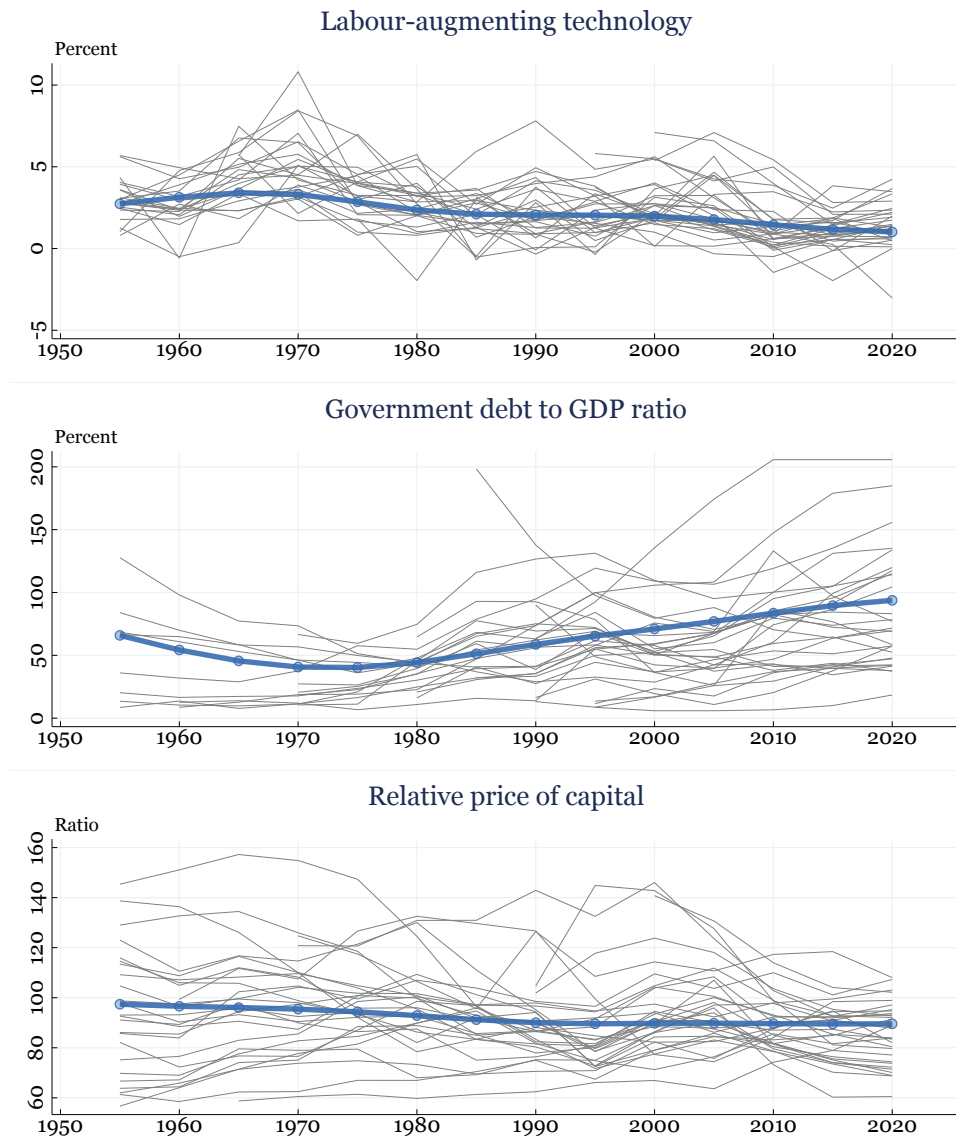
*Description:* Ratio between the Price level of capital formation ( $p1_i$ ) and the Price level of household consumption ( $p1_c$ ). *Source:* Penn World Table 10.0.

*Aggregation:* Cross-sectional weighted average of country-specific data with time-varying GDP weights from PWT (expenditure-side real GDP at current PPPs, in mil. 2017US\$).

*Sample:* 1950-2019.

For each of the drivers described above, Figure [C.2](#) plots the country-specific (where available) raw data together with its global trend component — i.e., after having (i) aggregated the data into a global concept using time-varying GDP weights and (ii) extracted the trend component as explained in Section [3](#).

**Figure C.2** Structural Drivers: Raw Data & Common Trends



NOTE. The figure plots the raw data we use to construct the observable proxies for the exogenous processes that in the model drive changes in the global equilibrium real interest rate  $R^*$ . Gray lines plot country-specific data (where available), while the blue line with circles plots the common trend component of the raw data across countries. Sample period: five-year periods from 1955 to 2020, where ‘1955’ corresponds to the period 1951-1955, and ‘2020’ corresponds to the period 2016-2019. See details in the text.

## C.2 Structural Model: Data for Calibration

### Real return on capital

*Description:* The real after-tax return to capital is constructed as total after-tax capital income,

net of depreciation divided by the previous period's value of capital.

Source: Caballero et al. (2017).

Aggregation: US data.

Sample: 1955-2013.

### **Cohort-specific labor supply**

*Description:* Civilian labor force participation rate by age.

*Source:* US Census (<https://www.census.gov/topics/employment/labor-force.html>).

*Aggregation:* US data.

*Sample:* Average across three data points 1996, 2006, and 2016. *Adjustments:* For the age buckets where the data was not as granular as we required, we assumed that the labor participation remained constant across those age groups. This is true for the cohorts '25-29' and '30-34' (as we have data only for the '25-34' cohort), '35-39' and '40-44', and '45-49' and '50-54'. For age buckets '80-84', '85-89', '90-94', and '95-99', labor participation rates are calculated by assuming a linear downwards trend between the rate in '75-79' (the oldest age group observed in the data) and zero participation for the age bucket '100+'.

*Notes:* We employ US data because of its superior granularity in the cross-sectional dimension (i.e., across cohorts). We cross-checked the patterns we obtain with US data with cross-country data from the OECD (which has information for only three cohorts, namely '15-24', '25-54', and '55-64'), and obtain very similar profiles for labor force participation.

### **Capital to output ratio**

*Description:* Capital stock at constant 2017 national prices (in mil. 2017US\$ divided by Real GDP at constant 2017 national prices (in mil. 2017US\$).

*Source:* Penn World Table 10.0.

*Aggregation:* Cross-sectional weighted average of country-specific data with time-varying GDP weights from PWT (expenditure-side real GDP at current PPPs, in mil. 2017US\$).

*Sample:* 1950-2019.

## **C.3 VAR Model: Observables**

**Short-term interest rates.** *Description:* government bills or money market instruments.

*Source:* Jorda et al. (2017) and Eikon Refinitiv. *Sample:* 1900-2019. *Aggregation:* Country-specific data.

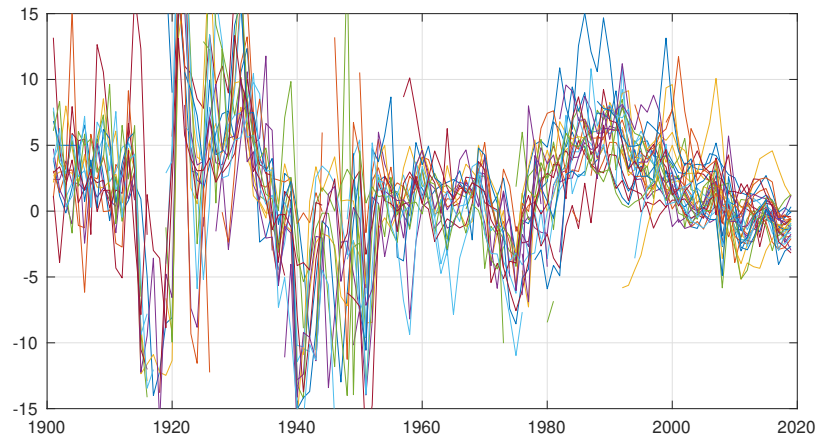
**Long-term interest rates.** *Description:* government bonds. *Source:* Jorda et al. (2017) and Eikon Refinitiv. *Sample:* 1900-2019. *Aggregation:* Country-specific data.

**Inflation rates.** *Description:* Log-difference of CPI index. *Source:* Jorda et al. (2017) and Eikon Refinitiv. *Sample:* 1900-2019. *Aggregation:* Country-specific data.

Figure C.3 reports the real interest rates (measured as nominal rates minus inflation) for the

31 countries in our sample.

**Figure C.3** Real Short-term Interest Rates Across Countries



NOTE. Each line displays the short-term real interest rate, computed as the short-term nominal interest rate minus inflation, for a given country. The y-axis in %. The sample period runs from 1900 to 2019.

## D Estimating Global $R^*$ Using a VAR with Common Trends

To obtain our empirical estimate of Global  $R^*$ , we use the approach developed by [Del Negro et al. \(2019\)](#), namely a vector autoregression (VAR) with common trends. The VAR allows to perform a multivariate trend-cycle decomposition and to extract the common trend component in real rates across countries. By imposing relatively uncontroversial restrictions on the long-run relations across variables (while remaining agnostic on whether these restrictions hold at shorter frequencies), we can interpret the estimated common trend in real interest rates across countries as the trend in the world real interest rate.

### D.1 VAR Model

The VAR with common trends is based on [Del Negro et al. \(2017\)](#) and [Del Negro et al. \(2019\)](#), so this appendix closely follows the exposition in those papers. The model we estimate is a state-space model with measurement equation given by:

$$y_t = \Lambda \bar{y}_t + \tilde{y}_t \quad (\text{D.1})$$

where  $y_t$  is an  $n \times 1$  vector of observables;  $\bar{y}_t$  is a  $\tau \times 1$  vector of trends;  $\tilde{y}_t$  is a  $n \times 1$  vector of stationary components;  $\Lambda$  is a  $n \times \tau$  matrix of loadings on which we impose restrictions based on economic theory (described below). The unobserved processes  $\bar{y}_t$  and  $\tilde{y}_t$  evolve according to a random walk and a VAR, respectively:

$$\bar{y}_t = \bar{y}_{t-1} + e_t \quad (\text{D.2})$$

$$\tilde{y}_t = \sum_{l=1}^p \Phi_l \tilde{y}_{t-l} + \varepsilon_t \quad (\text{D.3})$$

where  $\Phi_l$ 's are  $n \times n$  matrices of coefficients. The  $(\tau + n) \times 1$  vector of shocks  $(e_t', \varepsilon_t')$  is independently and identically distributed according to

$$\begin{pmatrix} e_t \\ \varepsilon_t \end{pmatrix} \sim \mathcal{N} \left( \begin{pmatrix} 0_\tau \\ 0_n \end{pmatrix}, \begin{pmatrix} \Sigma_e & 0 \\ 0 & \Sigma_\varepsilon \end{pmatrix} \right), \quad (\text{D.4})$$

with the  $\Sigma$ 's being conforming positive definite matrices, and where  $\mathcal{N}(\cdot)$  denotes the multivariate Gaussian distribution. Equations (D.2) and (D.3) represent the transition equations in the state-space model. The initial conditions  $\bar{y}_0$  and  $\tilde{y}_{0:-p+1} = (\tilde{y}'_0, \dots, \tilde{y}'_{-p+1})'$  are distributed according to

$$\bar{y}_0 \sim \mathcal{N}(\underline{y}_0, \underline{V}_0), \tilde{y}_{0:-p+1} \sim \mathcal{N}(0, V(\Phi, \Sigma_\varepsilon)), \quad (\text{D.5})$$

where  $V(\Phi, \Sigma_\varepsilon)$  is the unconditional variance of  $\tilde{y}_{0:-p+1}$  implied by (D.3). The priors for the VAR coefficients  $\Phi = (\Phi_1, \dots, \Phi_p)'$  and the covariance matrices  $\Sigma_\varepsilon$  and  $\Sigma_e$  have standard form, namely

$$p(\varphi | \Sigma_\varepsilon) = \mathcal{N}(\text{vec}(\Phi)\Sigma_\varepsilon \otimes \underline{\Omega}) \mathcal{I}(\varphi) \quad (\text{D.6})$$

$$p(\Sigma_\varepsilon) = \mathcal{IW}(\kappa_\varepsilon, (\kappa_\varepsilon + n + 1) \underline{\Sigma}_\varepsilon) \quad (\text{D.7})$$

$$p(\Sigma_e) = \mathcal{IW}(\kappa_e, (\kappa_e + \tau + 1) \underline{\Sigma}_e), \quad (\text{D.8})$$

where  $\varphi = \text{vec}(\Phi)$ ,  $\mathcal{I}(\varphi)$  is an indicator function which is equal to zero if the VAR is explosive and to one otherwise,  $\mathcal{IW}(\kappa, (\kappa + n + 1)\underline{\Sigma})$  denotes the inverse Wishart distribution with mode  $\underline{\Sigma}$  and  $\kappa$  degrees of freedom. The prior for  $\lambda$  is given by  $p(\lambda)$ , the product of independent Gaussian distributions for each element of the vector  $\lambda$ .

## D.2 Long-run Restrictions & Model Specification

Our baseline model includes data on the nominal yields of short-term ( $R_{it}$ ) and long-term ( $R_{it}^L$ ) government (or closely related) securities and inflation ( $\pi_{it}$ ) for each of the 31 countries in our sample, where  $i = 1, 2, \dots, 31$  denotes a country. As in Del Negro et al. (2019) we extract a country-specific and a common trend for each of the observables. Specifically, we extract  $(3 \times 31 + 3)$  trends from the cross-section of countries—a country-specific trend in inflation, the level of short-term interest rates, and the spread between long and short maturity rates; as well as a global trend in inflation, the level of short-term interest rates, and the spread between long and short maturity rates.

The key assumption imposed by Del Negro et al. (2019) to derive the long-run restrictions imposed on matrix  $\Lambda$  is the absence of arbitrage opportunities in the long run. In a simple asset-pricing framework, limits to arbitrage in the long-run imply the existence of a unique stochastic discount factor that prices all assets once their returns are exchange rate adjusted. Such unique stochastic discount factor, in turn, implies a common factor in country-specific interest rates, i.e. Global  $R^*$ .<sup>33</sup>

Specifically, the model we estimate is

$$R_{i,t} = \bar{r}_t^w + \bar{r}_t^i + \lambda_i^\pi \bar{\pi}_t^w + \bar{\pi}_t^i + \tilde{R}_{i,t}, \quad (\text{D.9})$$

$$R_{i,t}^L = \bar{r}_t^w + \bar{r}_t^i + \bar{t}s_t^w + \bar{t}s_t^i + \lambda_i^\pi \bar{\pi}_t^w + \bar{\pi}_t^i + \tilde{R}_{i,t}^L, \quad (\text{D.10})$$

$$\pi_{i,t} = \lambda_i^\pi \bar{\pi}_t^w + \bar{\pi}_t^i + \tilde{\pi}_{i,t}, \quad (\text{D.11})$$

for  $i = 1, 2, \dots, 31$ , and where  $\bar{R}_{it} - \bar{\pi}_{it} = \bar{r}_t^w + \bar{r}_t^i$ ;  $\bar{\pi}_{it} = \lambda_i^\pi \bar{\pi}_t^w + \bar{\pi}_t^i$ ; and  $R_{it}^L - R_{it} = \bar{t}s_t^w + \bar{t}s_t^i$ .

<sup>33</sup>The additional assumptions are that (i) the growth rate in the real exchange rate has no trend, a weaker than purchasing power parity in the long run; and (ii) the joint second moments of the variables that enter the Euler equations have no trend. See Del Negro et al. (2019) for more details.

The system is estimated jointly for all 31 countries in the sample (so  $n = 93$  and  $\tau = 96$ , as we have both global and country-specific trends).

### D.3 Priors and Initial Conditions

As in [Del Negro et al. \(2019\)](#), the prior for the VAR parameters  $\varphi$  is a standard Minnesota prior with the hyperparameter for the overall tightness equal to the commonly used value of 0.2 (see [Giannone et al., 2015](#)). The only exception is the ‘own-lag’ parameter which is centered at zero rather than one. The prior for the covariance  $\Sigma_\varepsilon$  of the innovations to the cycles  $\tilde{y}_t$ , is a relatively diffuse inverse Wishart distribution with degrees of freedom ( $\kappa_\varepsilon = n + 2$ ). The prior mean is set to be a diagonal matrix, with square root equal to 2, with the exception of the inflation cycle. Its prior mean is set to 4, to reflect the belief that nominal cycles might be more volatile than the other cycles.

We set the prior for  $\Sigma_e$ , the variance-covariance matrix of the innovations to all (common and country-specific) trends  $\bar{y}_t$ , to have a mode equal to a diagonal matrix with elements equal to 0.007 for all the real trends. This prior implies that the expected change in the trend over 100 years has a standard deviation equal to 0.7 percent. For the inflation trends, we use a value equal to  $2 \times 0.007$ , implying that the expected change in the trend over 50 years has a standard deviation equal to 0.7 percent. The degree of freedom is set to  $\kappa_e = 400$ .

We set the initial conditions to 4.7 percent for the real rate, 3.2 percent for inflation, and 0 percent for the term spread, in line with the sample averages over the period 1900 to 1920. As in [Del Negro et al. \(2019\)](#), the standard deviation for the initial conditions is set to 2 for the world inflation trend and 1 for all the others. The initial conditions for the country-specific trends have mean zero and standard deviations equal to half the value of the corresponding world counterparts.

All results are based on 10,000 simulations, of which we discard the first 2,500 as burn-in draws.<sup>34</sup>

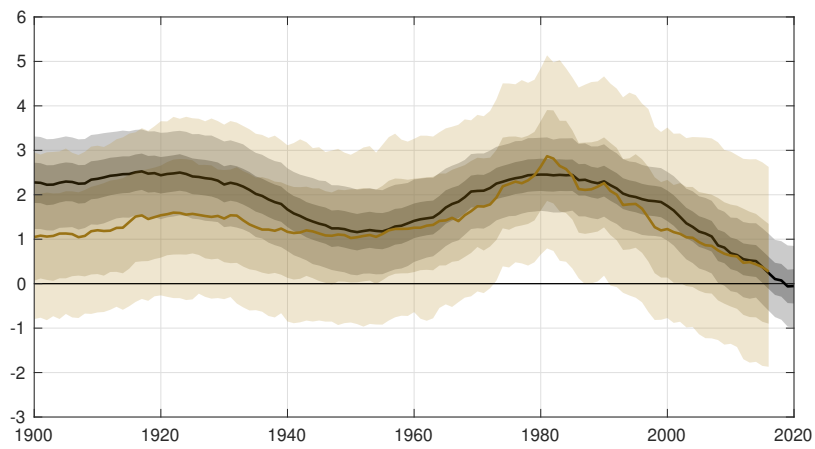
### D.4 Additional Results

This section provides additional results on our VAR estimate of Global  $R^*$ . A comparison with the original estimates by [Del Negro et al. \(2019\)](#) is reported in [Figure D.1](#). The Figure shows that extending the model from 7 to 31 countries leads to a very similar posterior median, but allows us to obtain substantially more precise estimates of  $R^*$ , as shown by the narrower posterior coverage intervals.

---

<sup>34</sup>The Gibbs sampler is described in Appendix A of [Del Negro et al. \(2017\)](#).

**Figure D.1** Baseline  $R^*$  Estimate Vs. Del Negro et al. (2019) Estimate



NOTE. The black line and shaded areas show the posterior median and the 68 and 95 percent posterior intervals of the VAR estimate of Global  $R^*$  presented in Appendix D and based on data for 31 countries. The yellow line and shaded areas display the estimates from the same model based on data for the G7 as in Del Negro et al. (2019). The y-axis is in %.

## E Possible Additional Drivers of Global $R^*$

The structural model brings together five key drivers of Global  $R^*$  within a single framework. Nonetheless, there are several potential influences on Global  $R^*$  that are not captured by our simulations. Estimating the long-run global trend of each driver for our simulation requires data on a large panel of countries over several decades. So in many cases we cannot include potential drivers within our simulations because the required data is not available. In this section, we outline some of these key missing drivers, drawing on existing research to discuss the likely mechanisms and qualitative effects on Global  $R^*$ .

**Competition.** There is a growing literature documenting a secular decline in the competitiveness of production, and a rise in monopolistic rents, particularly in the United States (De Loecker et al., 2020), but also globally (De Loecker and Eeckhout, 2018; Diez et al., 2018).

In our model, this effect could be captured by an increase in the mark-up,  $\mu$ , over time. In partial equilibrium, such an increase would reduce the demand for capital, thereby putting downward pressure on the equilibrium real interest rate. However, the general-equilibrium effect of this change would depend on how the resulting profits are distributed to households. If they are distributed proportionally to labor income, an increase in profits would raise the desired savings of these households, pushing down on the interest rate. Conversely, if profits are distributed proportionally to wealth and capital income, an increase in profits would effectively “crowd out” desired savings in the capital stock, and hence push up on the equilibrium real interest rate.<sup>35</sup>

Eggertsson et al. (2019) assume a rise in mark-ups from 14% to 25% between 1970 and 2015, calibrated to match the decline in the labor share in the United States. They assume that profits are distributed proportionally to labor income, and estimate that this 11 percentage point change reduced the equilibrium real interest rate by around 0.5pp, suggesting a potentially large effect of changes in competition. Using data for 134 countries, De Loecker and Eeckhout (2018) estimate a large rise in mark-ups, from around 10% to 60% between 1980 and 2016.<sup>36</sup>

Consistent global data on mark-ups from 1950 is difficult to obtain, making it challenging to formally incorporate this driver in our simulations. While an increase in the mark-up would likely have a large impact on the simulated path of Global  $R^*$ , the direction of the effect is ambiguous without further information on how the resulting profits are distributed.

---

<sup>35</sup>In fact, allowing agents to buy claims to future firm profits would lead to households endogenously using these claims as an additional savings vehicle for retirement, pushing up on  $R^*$  even more than a case where profits are exogenously distributed to wealthier households. For further explanation of this point, see Lisack et al. (2017).

<sup>36</sup>Using data for 74 countries over the same time period, Diez et al. (2018) find that increases in mark-ups appear to have been concentrated in advanced economies, with net mark-ups rising from close to 0 in 1980 to around 0.4 in 2016. In contrast, mark-ups in emerging economies are estimated to have been relatively stable.

**Rising retirement age.** As people live longer, they are likely to work until later in life, either endogenously through increased labor supply in old age, or through a rise in statutory retirement ages. For example, in 2021 the OECD reported that normal retirement ages were set to rise in a majority of OECD countries (OECD, 2021, page 13).

These changes could, in principle, be incorporated in our simulations through changes in the life-cycle profile of age-specific labor supply,  $\rho_\tau$ . Other things equal, a longer working life flattens out the life-cycle profile of labor income, reducing the incentive to accumulate assets in order to smooth consumption. This would push up on the equilibrium real interest rate, effectively offsetting some of the downward pressure from increased longevity.

Again, consistent data on age-specific labor supply over time for our large panel of countries is not readily available. Moreover, even if this data were available, the effect through this channel may not be very large.<sup>37</sup> Using a similar model to ours, Lisack et al. (2021) find that even a five-year increase in the retirement age, coupled with an assumption that households remain highly productive throughout old age, is not sufficient to offset the downward pressure on the equilibrium real interest rate from increased longevity.<sup>38</sup> Even under these assumptions, the additional labor income from a longer working life is small in comparison to the substantial increase in the proportion of life spent in retirement.

**Risk and risk aversion.** Changes to the quantity or price of risk would lead to an increase in the risk premium, which would push down on the risk-free rate,  $R^*$ , for a given return to capital. Indeed, there is evidence that an increase in the ‘convenience yield’, the premium on government bonds capturing their relative safety and liquidity, has played a significant role in the decline in safe rates of return both in the United States (Del Negro et al., 2017) and globally (Del Negro et al., 2019).

Though the model does not include risk, there is a fixed wedge between the risk-free rate and the return to capital,  $\phi$ . In a standard asset-pricing model, this wedge would be affected by both the quantity of risk (i.e., the volatility in the productivity of capital) and the price of risk (i.e., the risk aversion of households). Therefore, in principle, changes in the risk premium over time could be incorporated in our simulations via time variation in  $\phi$ . While quantifying this effect is challenging, again due to the lack of data availability for our large panel of countries, it is likely that any secular rise in  $\phi$  would reduce Global  $R^*$  further.<sup>39</sup>

---

<sup>37</sup>Secular changes in broader provision of social security and social insurance by governments could have much larger effects on equilibrium real interest rates (Rachel and Summers, 2019).

<sup>38</sup>This is a large increase in retirement age compared to current expectations: “Based on legislated measures, the normal retirement age will increase in the OECD on average by about two years in the next four decades, during which life expectancy in old age is projected to increase by about four years.” (OECD, 2021, page 12)

<sup>39</sup>Using US data, Caballero et al. (2017) find evidence of increasing risk premia from the 1980s. Not all estimates of risk premia, however, would suggest secular changes in  $\phi$ . For example, Gourinchas et al. (2022) estimate the drivers of the consumption to wealth ratio for several advanced economies from 1870.

**Health and social insurance.** Rachel and Summers (2019) argue that the widespread growth in the provision of publicly-financed social security and healthcare would both reduce the incentives for households to accumulate wealth and crowd out private capital, resulting in upward pressure on Global  $R^*$ . By combining the results from two structural models, they estimate that this trend may have increased Global  $R^*$  by 2–3pp between 1970 and 2015.<sup>40</sup>

**Inequality.** There is a large literature documenting a rise in inequality over recent decades, focused on the United States but also in other countries (Alvaredo et al., 2017).

A rise in inequality could potentially affect the equilibrium real interest rate through two channels. First, if increased inequality is caused by an increase in the dispersion of income, this implies higher individual income risk, inducing higher precautionary savings, thereby reducing the real interest rate (Auclert and Rognlie, 2018). Auclert and Rognlie (2017) find that a doubling of the share of labor income earned by the top 1%, in the United States since the 1980s, can account for between 0.45 and 0.85 percentage points decline in the real interest rate. A second channel operates through changes in the composition of the population towards high-income households, who have the highest savings rates. Mian et al. (2021) show that this channel has significantly increased aggregate savings in the United States in recent decades, consistent with the decline in  $R^*$ .<sup>41</sup>

While our model incorporates heterogeneity across age groups, there is no within-cohort heterogeneity. Cross-country and long-run data on household-level income and savings is not readily available, making it very difficult to incorporate either channel. However, both channels suggest that a rise in inequality is likely to exert downward pressure on the equilibrium real interest rate.

---

Their estimates suggest a minor role for the risk premium (much smaller than the safe rate), with no strong trend over time.

<sup>40</sup>When accounting for all factors, including some of those considered in the current paper, Rachel and Summers (2019) estimate that Global  $R^*$  fell by around 3pp over this period.

<sup>41</sup>Moll et al. (2021) propose an alternative mechanism where inequality results from an increase in automation, which also leads to an increased wedge between the return to capital and the safe interest rate.